Recent Results of the Tibet ASγ Experiment

Sei Kato
(Institut d'Astrophysique de Paris)

The picture taken from https://www.icrr.u-tokyo.ac.jp/news/10202/

Tibet ASγ Collaboration

M. Amenomori[1], M. Anzorena[2], Y. W. Bao[3], X. J. Bi[4], D. Chen[5], T. L. Chen[6], W. Y. Chen[4], Xu Chen[5], Y. Chen[3], Cirennima[6], S. W. Cui[7], Danzengluobu[6], L. K. Ding[4], J. H. Fang[4,8], K. Fang[4], C. F. Feng[9], Y. L. Feng[6], Zhaoyang Feng[4], Z. Y. Feng[10], K. Fujita[2], Qi Gao[6], Q. B. Gou[4], R. Garcia[2], Y. Q. Guo[4], Y. Y. Guo[4], C. Y. Han[11], Y. Hayashi[12], H. H. He[4], Z. T. He[7], K. Hibino[13], N. Hotta[14], Haibing Hu[6], H. B. Hu[4], K. Y. Hu[4,8], J. Huang[4], G. Imaizumi[2], H. Y. Jia[10], L. Jiang[4], P. Jiang[5], H. B. Jin[5],K. Kasahara[15], Y. Katayose[16], C. Kato[12], S. Kato[17], T. Kawashima[2], K. Kawata[2], M. Kozai[18], Labaciren[6], G. M. Le[19], A. F. Li[20,10,4], H. J. Li[6], W. J. Li[4,10], Y. Li[5], Y. H. Lin[4,8], B. Liu[21], C. Liu[4], J. S. Liu[4], L. Y. Liu[5], M. Y. Liu[6], W. Liu[4], H. Lu[4], T. Makishima[16], Y. Masuda[12], S. Matsuhashi[16], M. Matsumoto[12], X. R. Meng[6], Y. Meng[4,8], A. Mizuno[2], K. Munakata[12], Y. Nakamura[2], H. Nanjo[1], C. C. Ning[6], M. Nishizawa[22], Y. Noguchi[16], M. Ohnishi[2], S. Okukawa[16], S. Ozawa[23], X. Qian[5], X. L. Qian[24], X. B. Qu[25], T. Saito[26], M. Sakata[27], T. Sako[2], T. K. Sako[28], J. Shao[4,10], Q. Q. Shi[11], T. Shibasaki[29], M. Shibata[16], A. Shiomi[29], F. Sugimoto[2], H. Sugimoto[30], W. Takano[13], M. Takita[2], Y. H. Tan[4],N. Tateyama[13], S. Torii[31], H. Tsuchiya[32], S. Udo[13], R. Usui[16], H. Wang[4], S. Wang[11], S. F. Wang[6], Y. P. Wang[6], Wangdui[6], H. R. Wu[4], Q. Wu[6], J. L. Xu[5], L. Xue[9], G. Yamagoshi[16], Z. Yang[4], Y. Q. Yao[5], J. Yin[5], Y. Yokoe[2], Y. L. Yu[4,8], A. F. Yuan[6], L. M. Zhai[5], H. M. Zhang[4], J. L. Zhang[4], X. Zhang[3], X. Y. Zhang[9], Y. Zhang[4], Yi Zhang[33], Ying Zhang[4], S. P. Zhao[4], Zhaxisangzhu[6], X. X. Zhou[10]

1 Department of Physics, Hirosaki Univ., Japan.
2 Institute for Cosmic Ray Research, Univ. of Tokyo, Japan.
3 School of Astronomy and Space Science, Nanjing Univ., China.
4 Key Laboratory of Particle Astrophysics, Institute of High Energy Physics, CAS, China.
5 National Astronomical Observatories, CAS, China.
6 The Key Laboratory of Cosmic Rays (Tibet Univ.), Ministry of Education, China.
7 Department of Physics, Hebei Normal Univ., China.
8 Univ. of Chinese Academy of Sciences, China.
9 Institute of Frontier and Interdisciplinary Science and Key Laboratory of Particle Physics and Particle Irradiation (MOE), Shandong Univ., China.
10 Institute of Modern Physics, SouthWest Jiaotong Univ., China.
11 Shandong Key Laboratory of Optical Astronomy and Solar-Terrestrial Environment, School of Space Science and Physics, Institute of Space Sciences, Shandong Univ., China.
12 Department of Physics, Shinshu Univ., Japan.
13 Faculty of Engineering, Kanagawa Univ., Japan.
14 Faculty of Education, Utsunomiya Univ., Japan.
15 Faculty of Systems Engineering, Shibaura Institute of Technology, Japan.
16 Faculty of Engineering, Yokohama National Univ., Japan.
17 Institut d'Astrophysique de Paris, CNRS UMR 7095, Sorbonne Université, France.
18 Polar Environment Data Science Center, Joint Support-Center for Data Science Research, Research Organization of Information and Systems, Japan.
19 National Center for Space Weather, China Meteorological Administration, China.
20 School of Information Science and Engineering, Shandong Agriculture Univ., China.
21 Department of Astronomy, School of Physical Sciences, Univ. of Science and Technology of China, China.
22 National Institute of Informatics, Japan.
23 National Institute of Information and Communications Technology, Japan.
24 Department of Mechanical and Electrical Engineering, Shangdong Management Univ., China.
25 College of Science, China Univ. of Petroleum, China.
26 Tokyo Metropolitan College of Industrial Technology, Japan.
27 Department of Physics, Konan Univ., Japan.
28 Department of Information and Electronics, Nagano Prefectural Institute of Technology, Japan.
29 College of Industrial Technology, Nihon Univ., Japan.
30 Shonan Institute of Technology, Japan.
31 Research Institute for Science and Engineering, Waseda Univ., Japan.
32 Japan Atomic Energy Agency, Japan.
33 Key Laboratory of Dark Matter and Space Astronomy, Purple Mountain Observatory, CAS, China.

Tibet Air Shower Array (1990 ~)

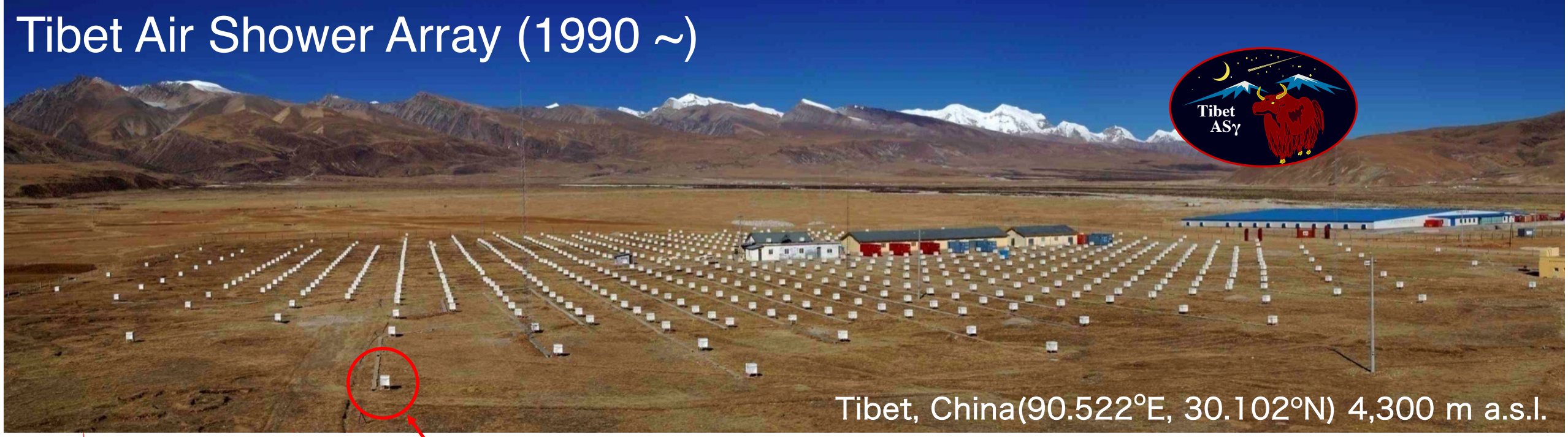

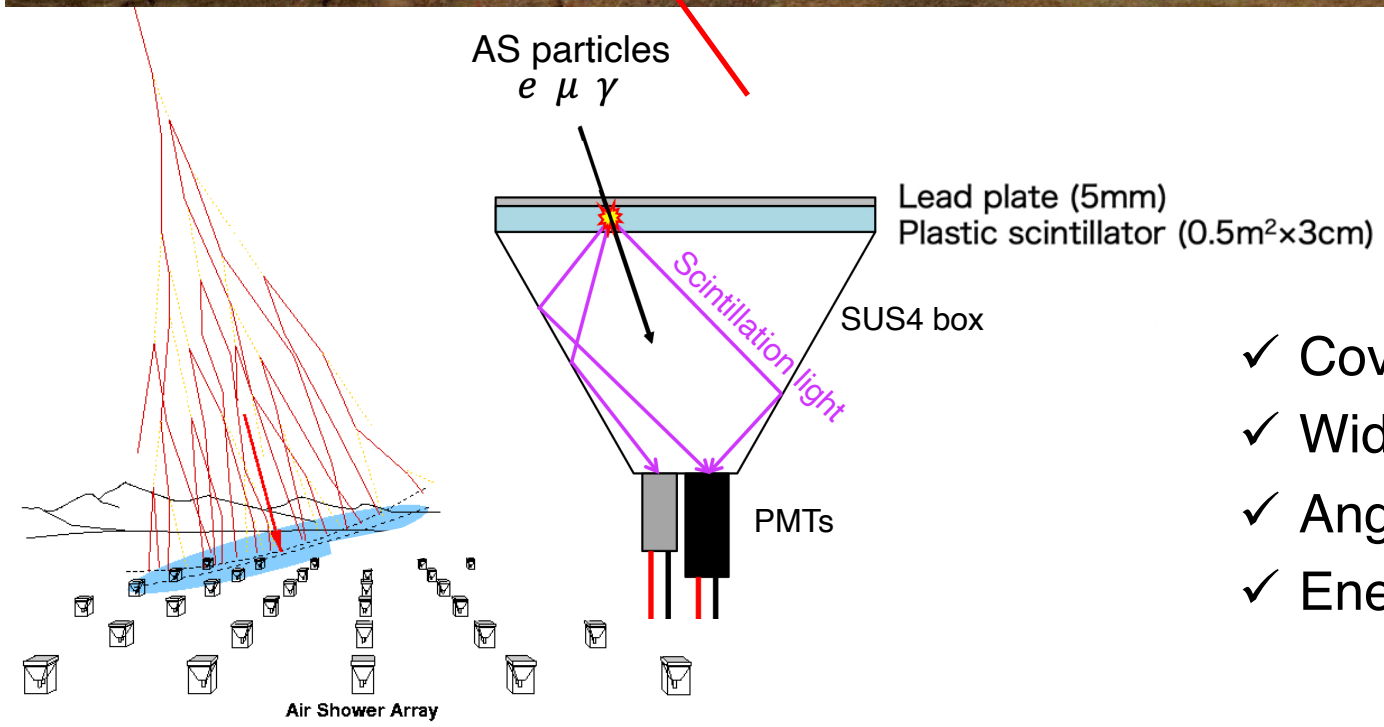

- ✓ Covering 65,700 m² with 600 scintillation detectors
- ✓ Wide F.O.V. (~ 2 sr) & high duty cycle (>90%)
- ✓ Angular resolution：0.2° for 100TeV γ
- ✓ Energy resolution：20% for 100TeV γ

Underground Muon Detector Array (2014 ~)

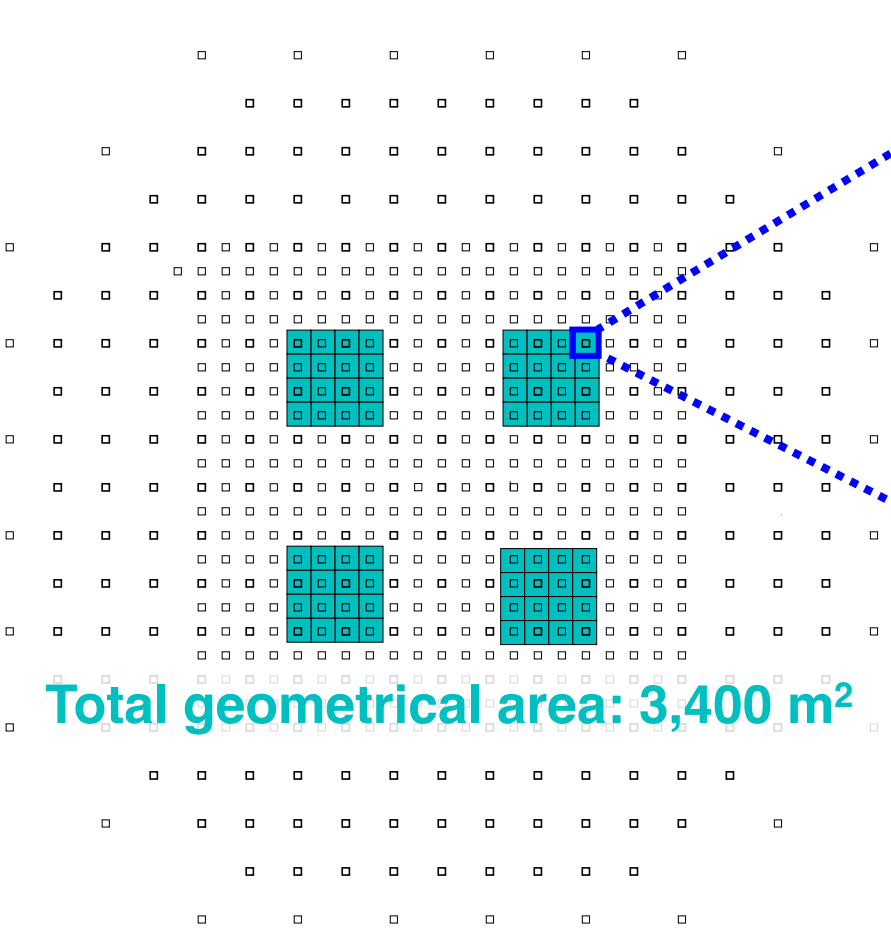

Total geometrical area: 3,400 m²

□ : Surface detectors

■ : Underground detectors

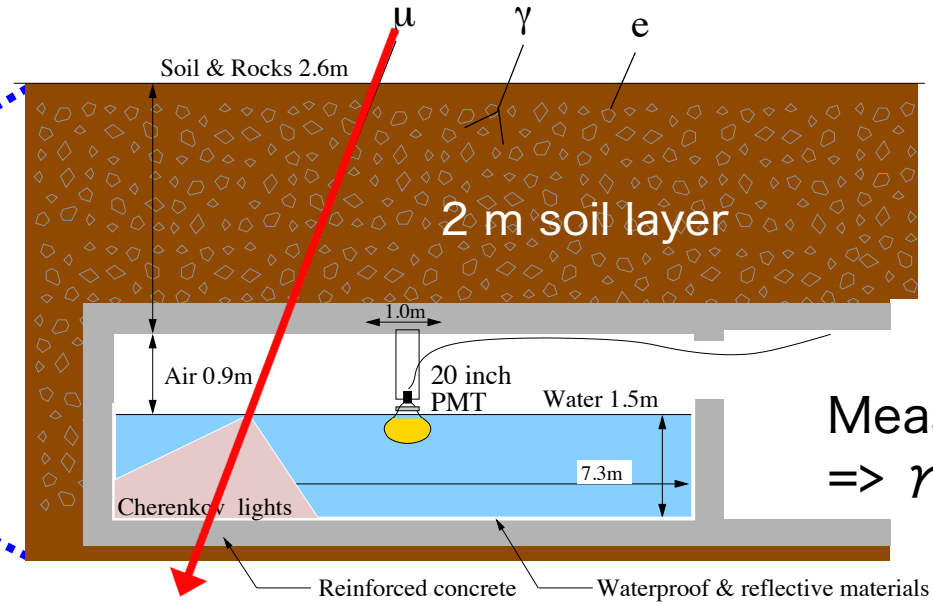

Measurement of muons
=> γ /hadron separation

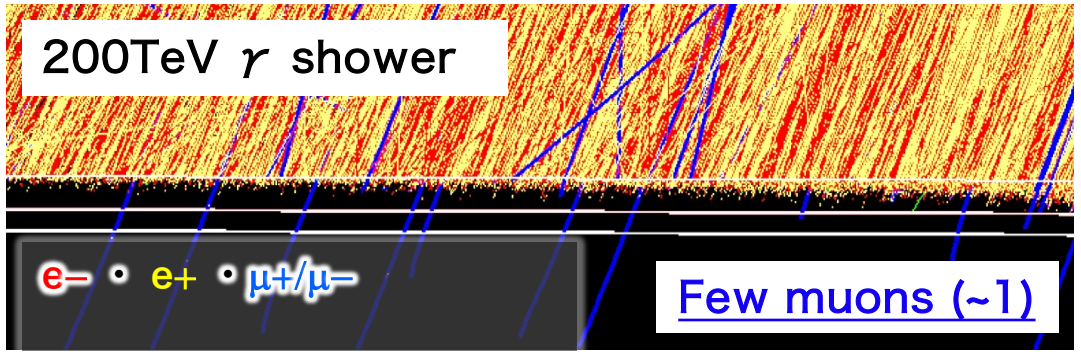

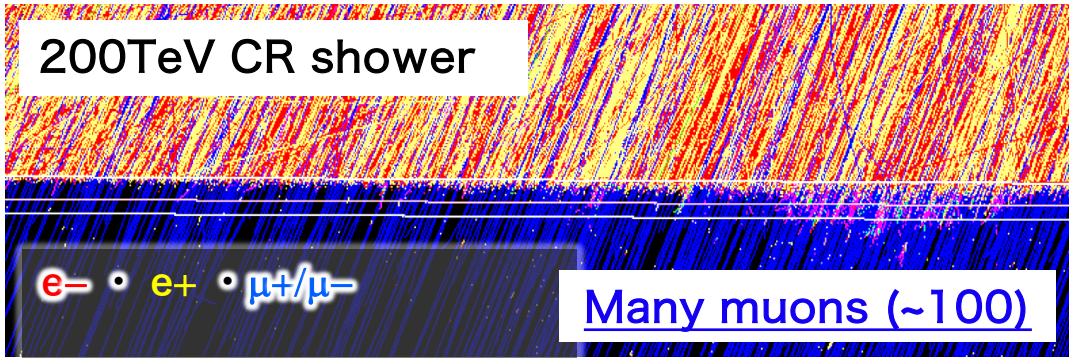

BG rejection : >99.9% @ sub-PeV
High sensitivity to γ rays

Sub-PeV γ-Ray Astronomy: Search for the Origin of PeV CRs

All particle CR spectrum

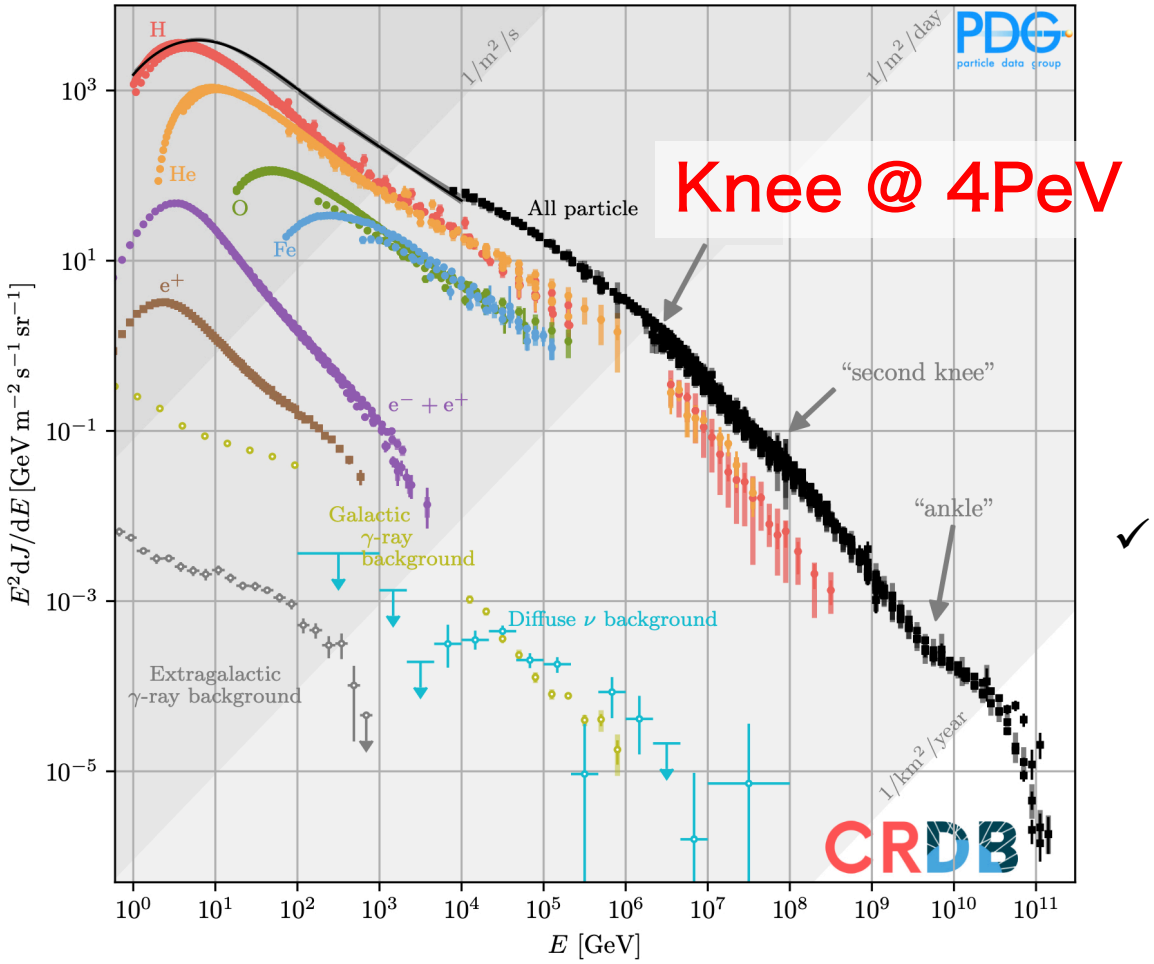

Navas et al. (PDG), PRD 110, 030001 (2024)

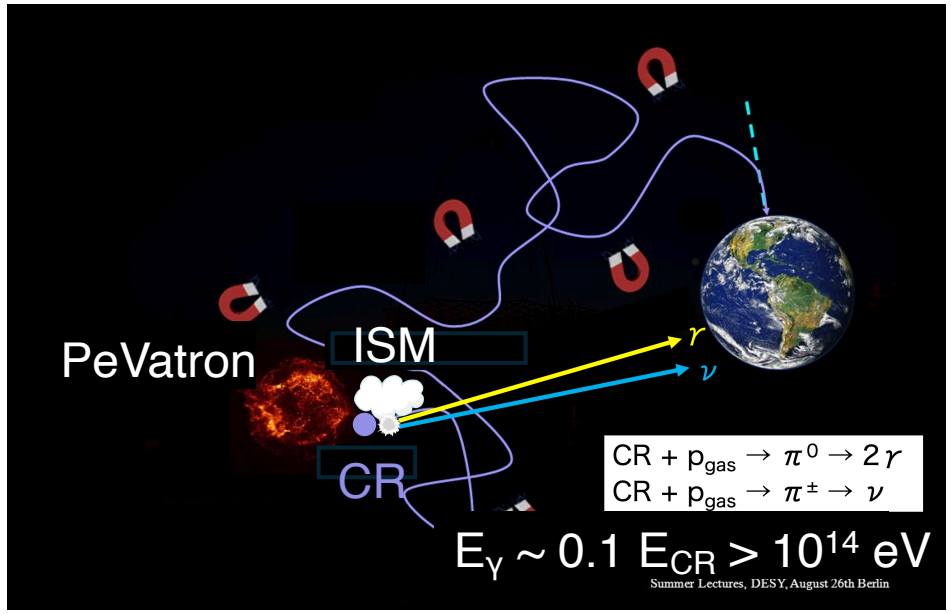

✓ Knee is dominated by light elements (LHAASO)

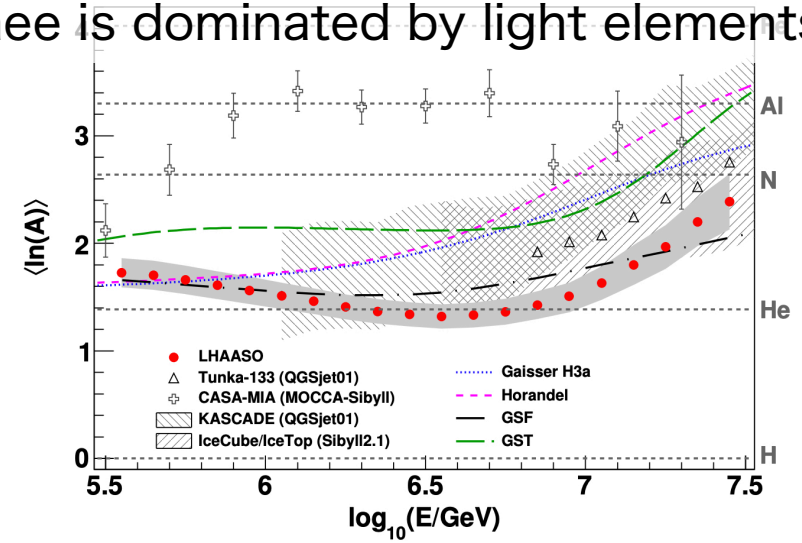

Cao et al., PRL 132, 131002 (2024)

Search for Galactic PeV CR proton accelerators: *PeVatrons*

Sub-PeV Gamma-Ray Astronomy by the Tibet ASγ Experiment (2019~)

1st Detection of Sub-PeV γ Rays from the Crab Nebula (2019)

Amenomori et al., PRL 123, 051105 (2019)

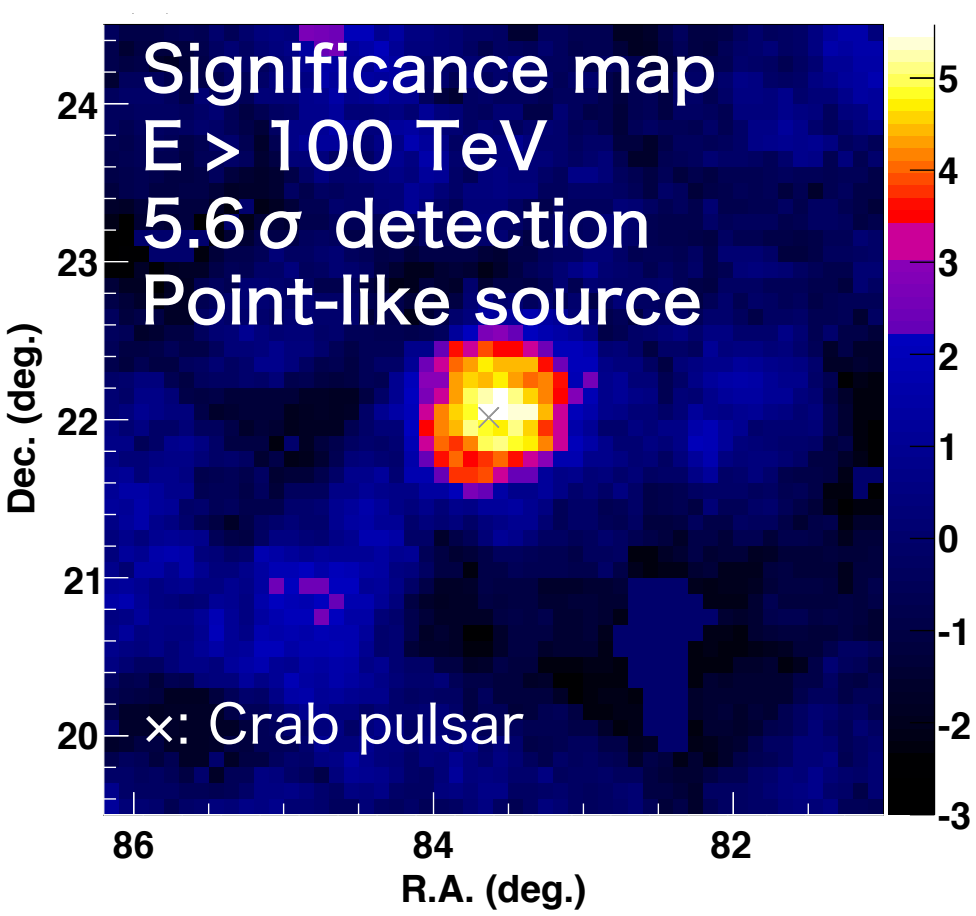

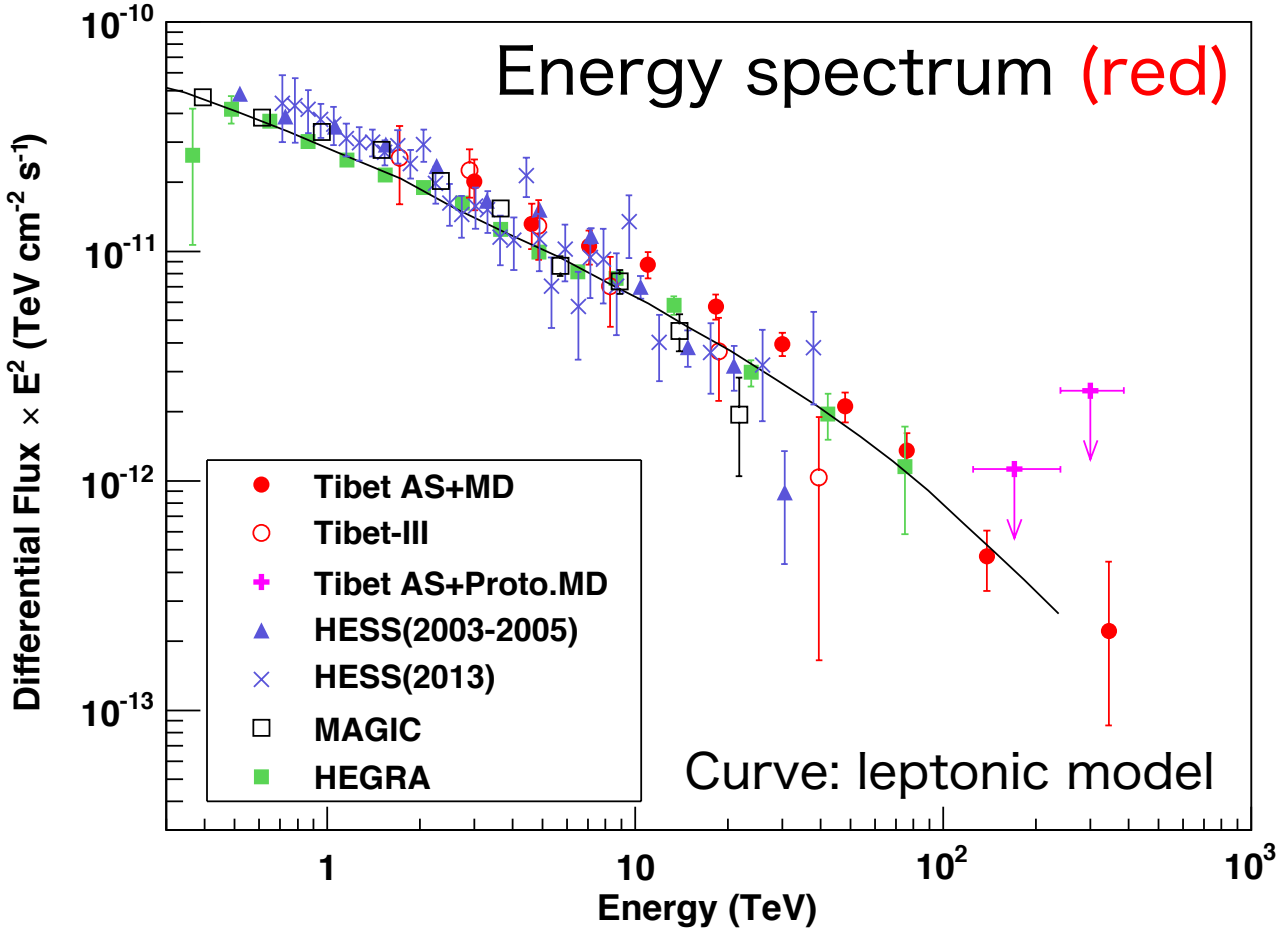

- ✓ $E_{\gamma,max}$ = 450 TeV (Now beyond 1 PeV by LHAASO)
- ✓ Consistent w/ ICS of electrons & CMB

Detection of a PeVatron Candidate：SNR G106.3+2.7 (2021)

Significance map @ E >10 TeV

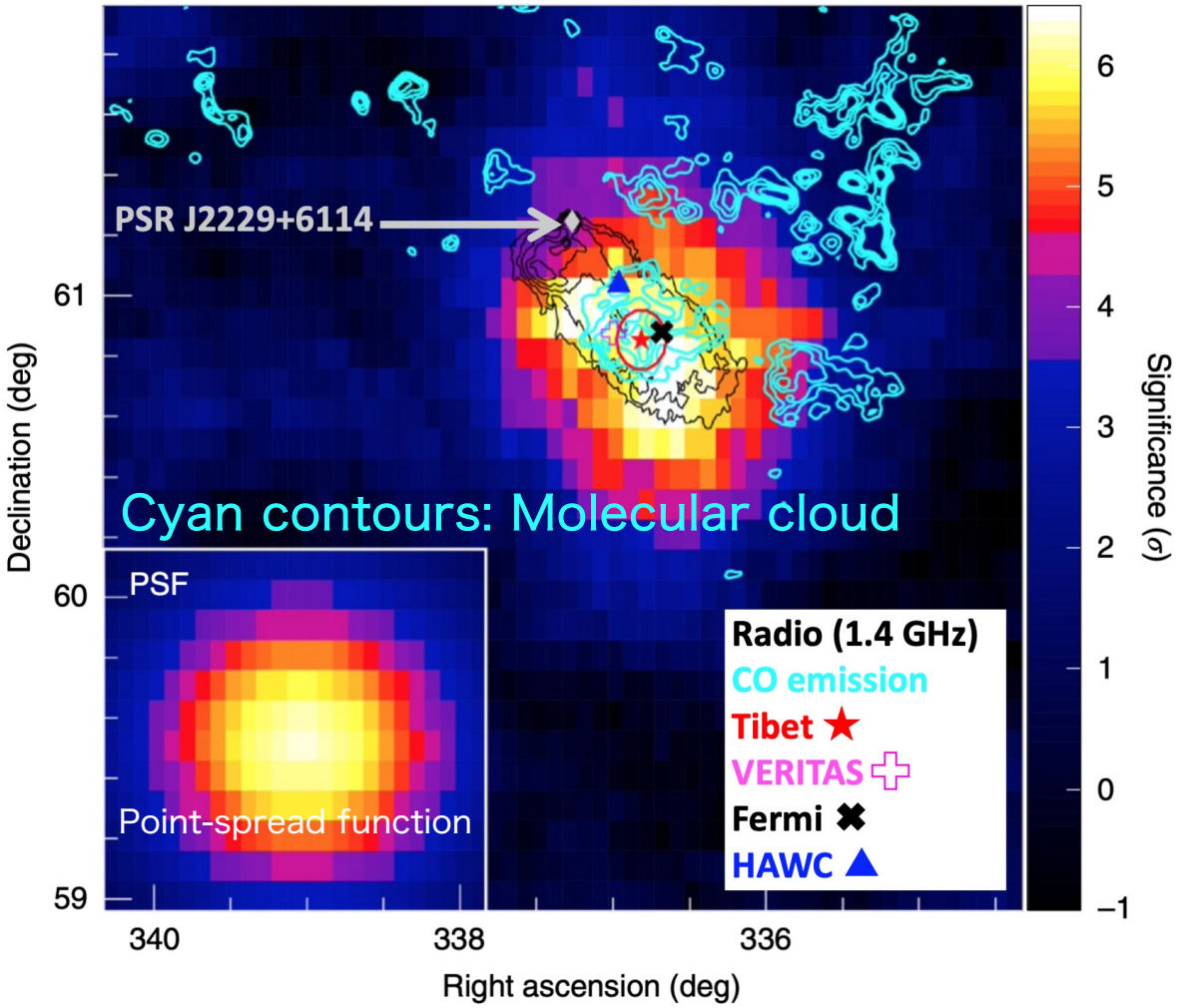

M. Amenomori et al., Nat. Astron. Lett, 5, 460 (2021)

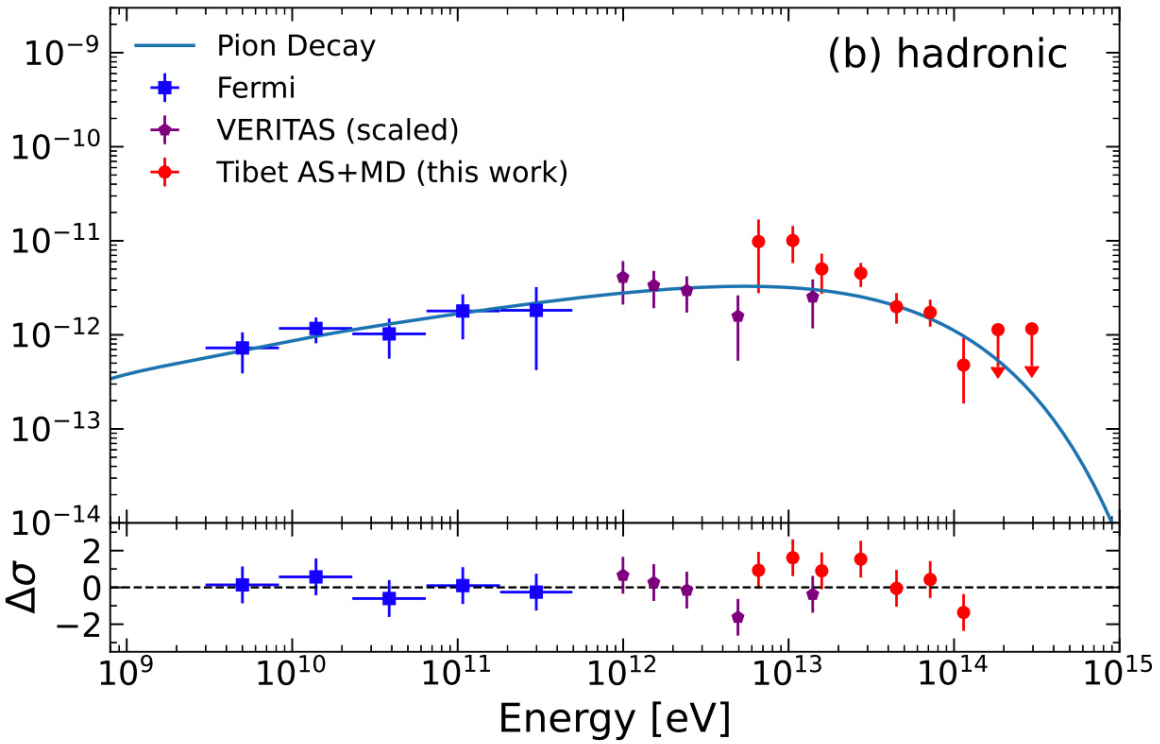

See also
Pineault & Joncas, Astron. J. **120**, 3218 (2000)
Albert et al., ApJL 896, 29 (2020)
Cao et al., Nature 594, 33 (2021)

- ✓ SNR G106: discovered in radio continuum (1.4GHz)
- ✓ Gamma-ray emission coming from a molecular cloud
- ✓ Hadronic modeling gives $E_{p,cut}$ ~ 500TeV

Multi-Wavelength Spectral Analysis of SNR G106.3+2.7

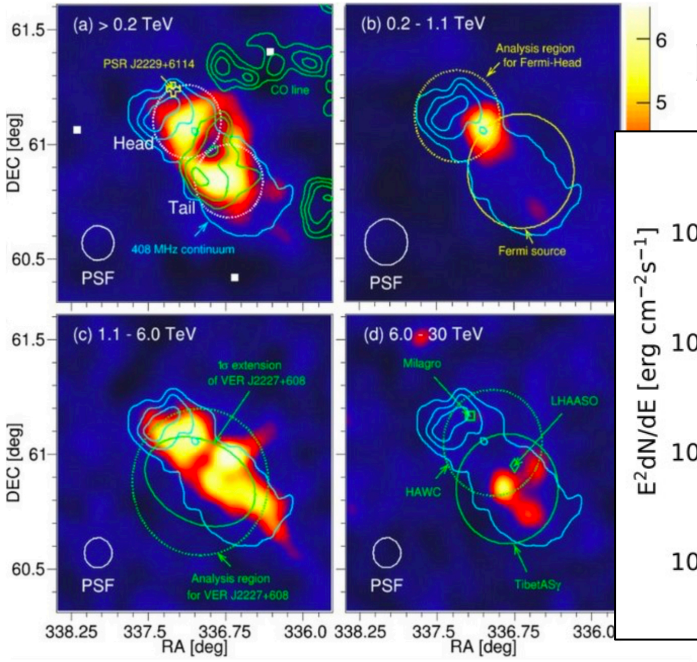

MAGIC Collab. A&A (2023)

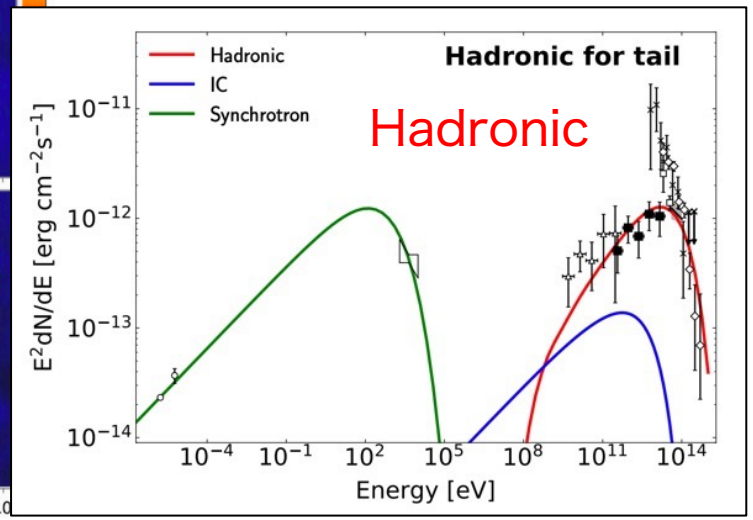

Fang et al., PRL (2022)

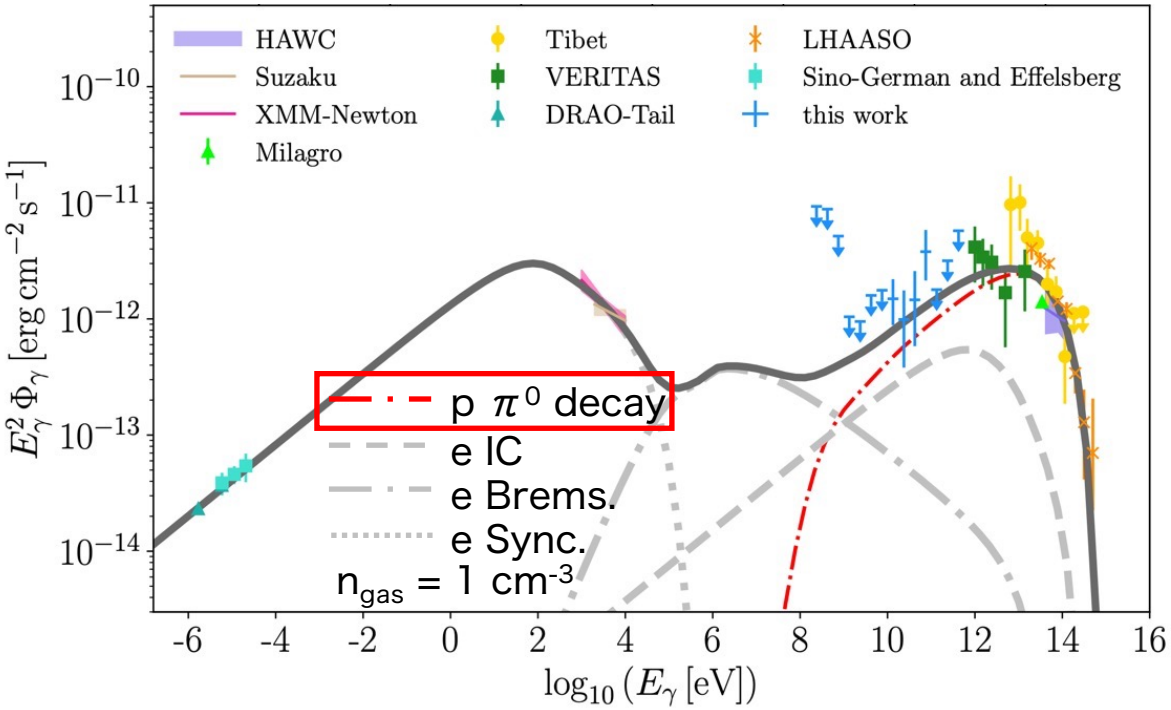

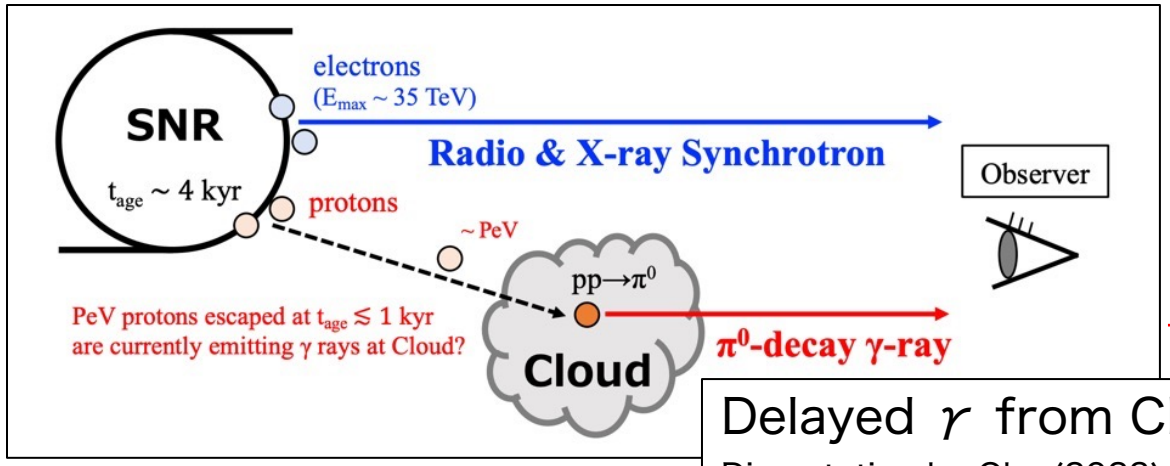

Delayed γ from CRp?
Dissertation by Oka (2023)

Hadronic emission needed @ GeV – 500TeV

Max. CR proton energy ~ 1PeV !!

Galactic Diffuse Gamma-Ray Emission (GDE, 2021)

Source gamma rays

Diffuse gamma rays

Extended along Gal. Plane &
No source counterpart

太陽系
Solar system

Galactic Diffuse Gamma-Ray Emission (GDE, 2021)

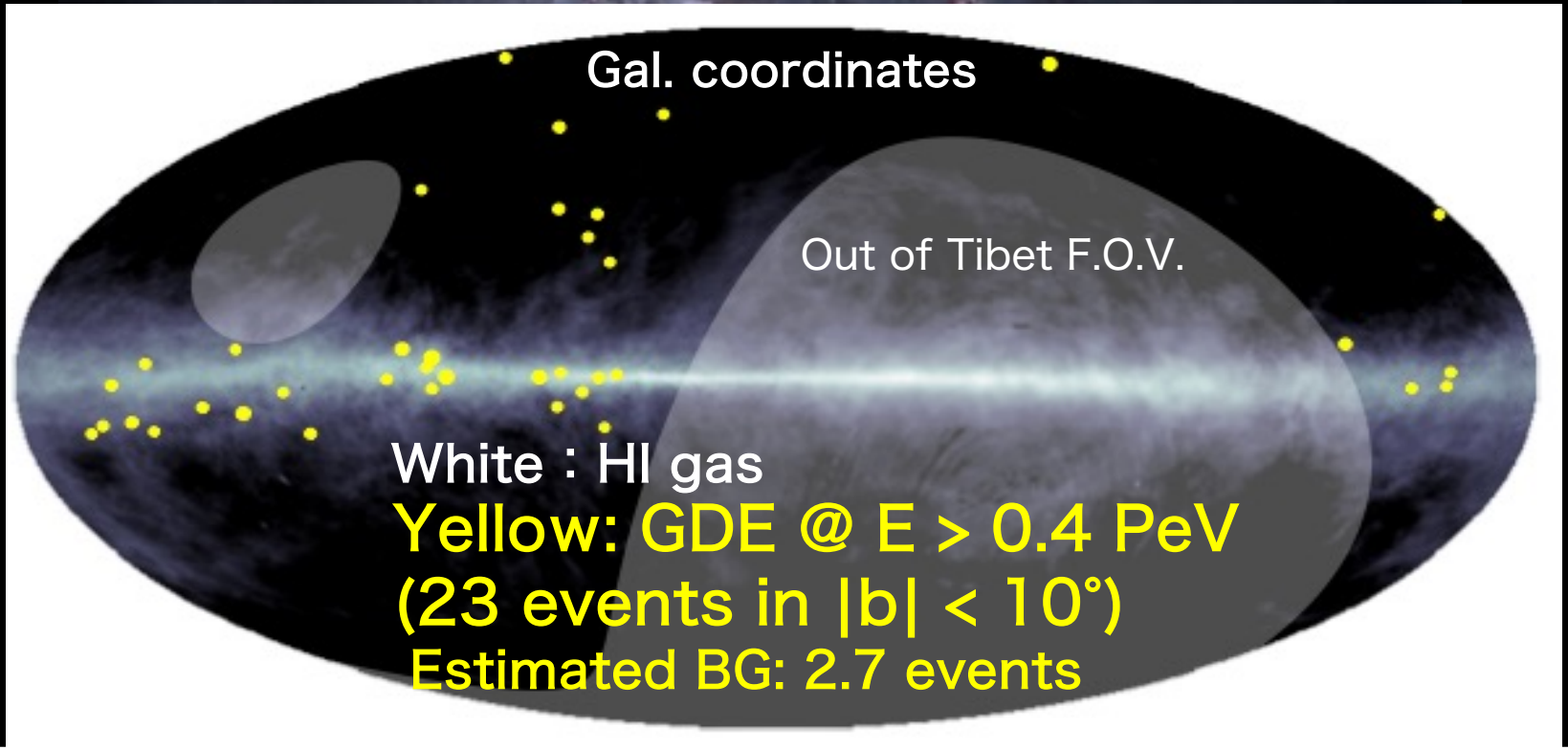

✓ First detection (6σ) of sub-PeV GDE
✓ Establishing the existence of Galactic PeVatrons

Amenomori et al., PRL 126, 141101 (2021)

Detection of Other Sub-PeV γ-Ray Sources

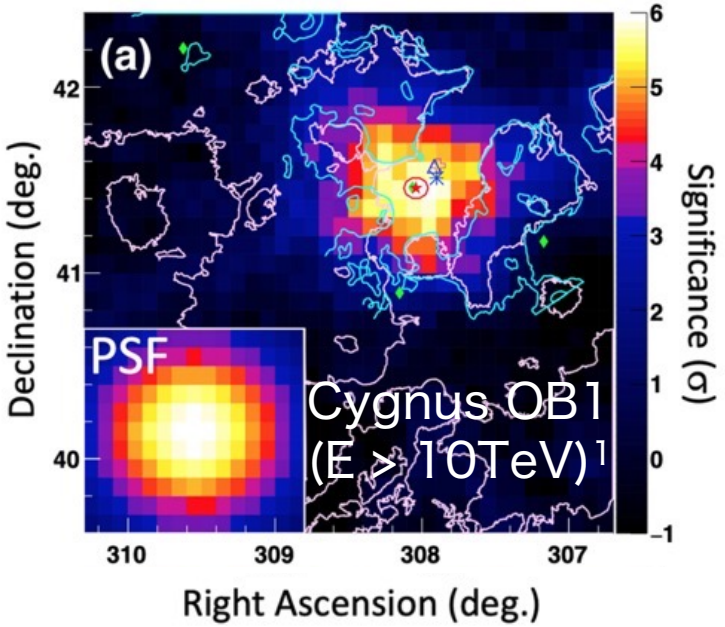

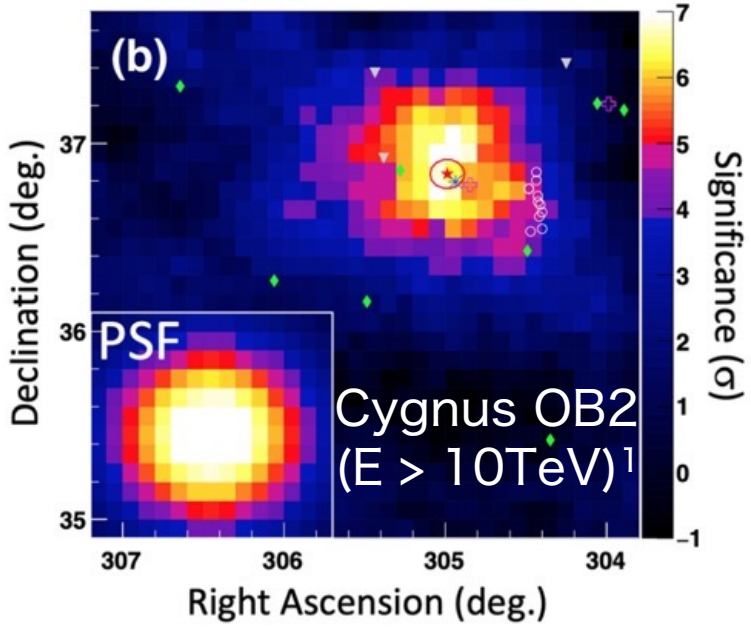

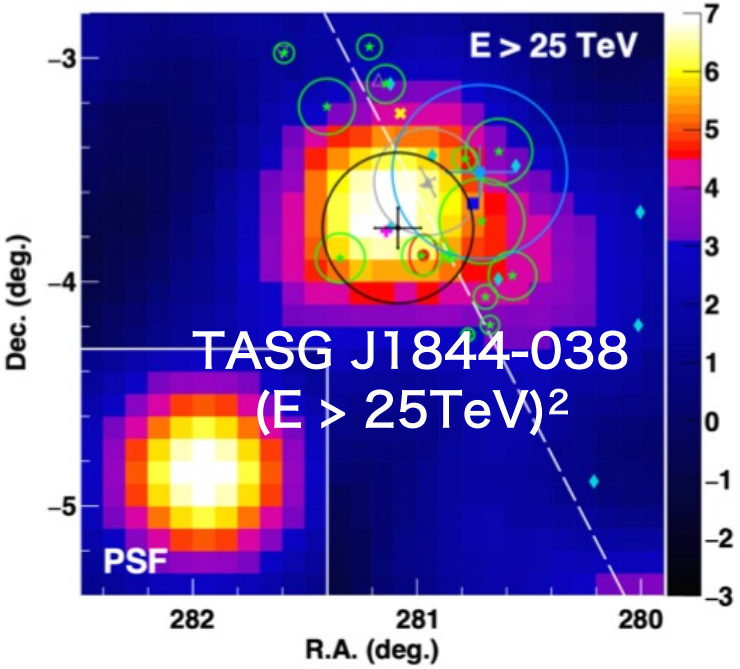

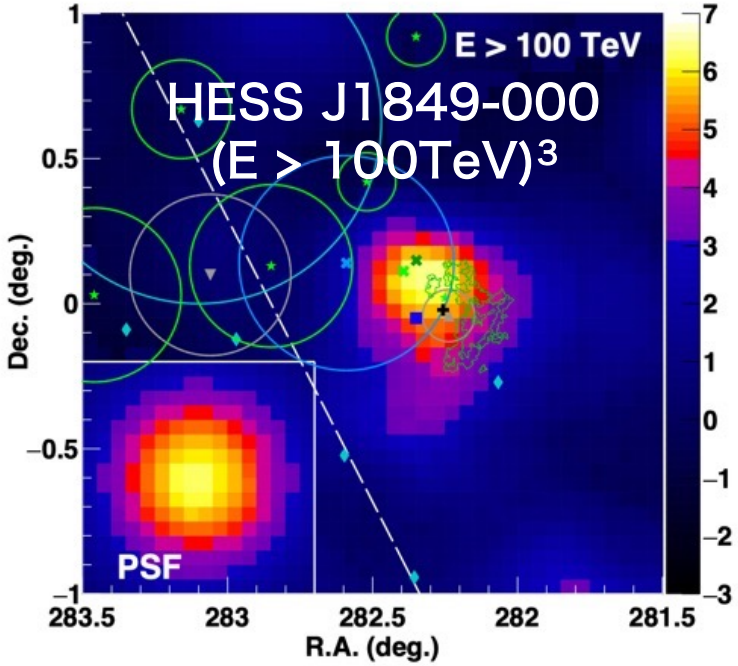

TASG J1844–038 &
HESS J1849–000
are PeVatron candidates[2,3]

1. Amenomori et al., PRL 127, 031102 (2021)
2. Amenomori, ⋯, S.K. et al., ApJ 932, 120 (2022)
3. Amenomori, ⋯, S.K. et al., ApJ 954, 200 (2023)

A Bit More about Galactic Diffuse γ Rays…

S.K. et al., ApJL 961, L13 (2024)
S.K. et al., ApJL 977, L3 (2024)
S.K. et al., ApJ 984, 98 (2025)

※These are NOT collaboration papers

Source Contamination of Tibet GDE?

GDE: Galactic diffuse (γ-ray) emission

Tibet GDE = True GDE + source contamination?

Modeling by Vecchiotti et al., ApJ 928, 19 (2022)

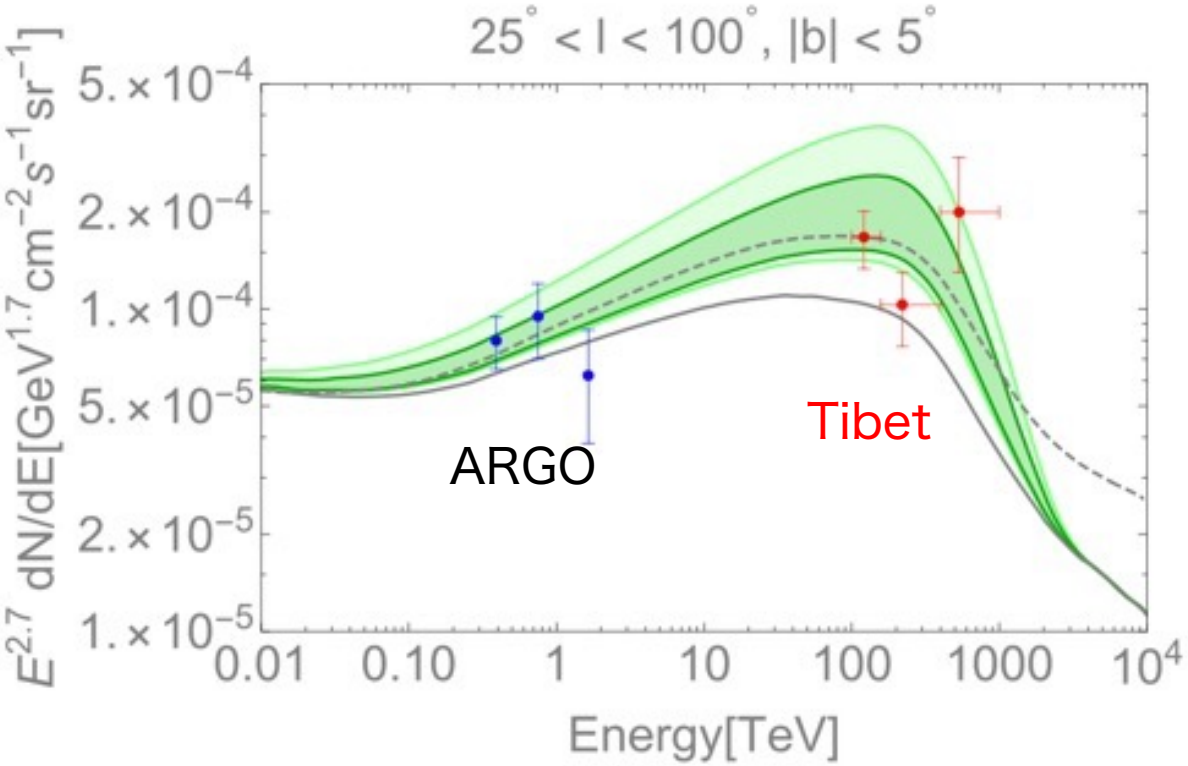

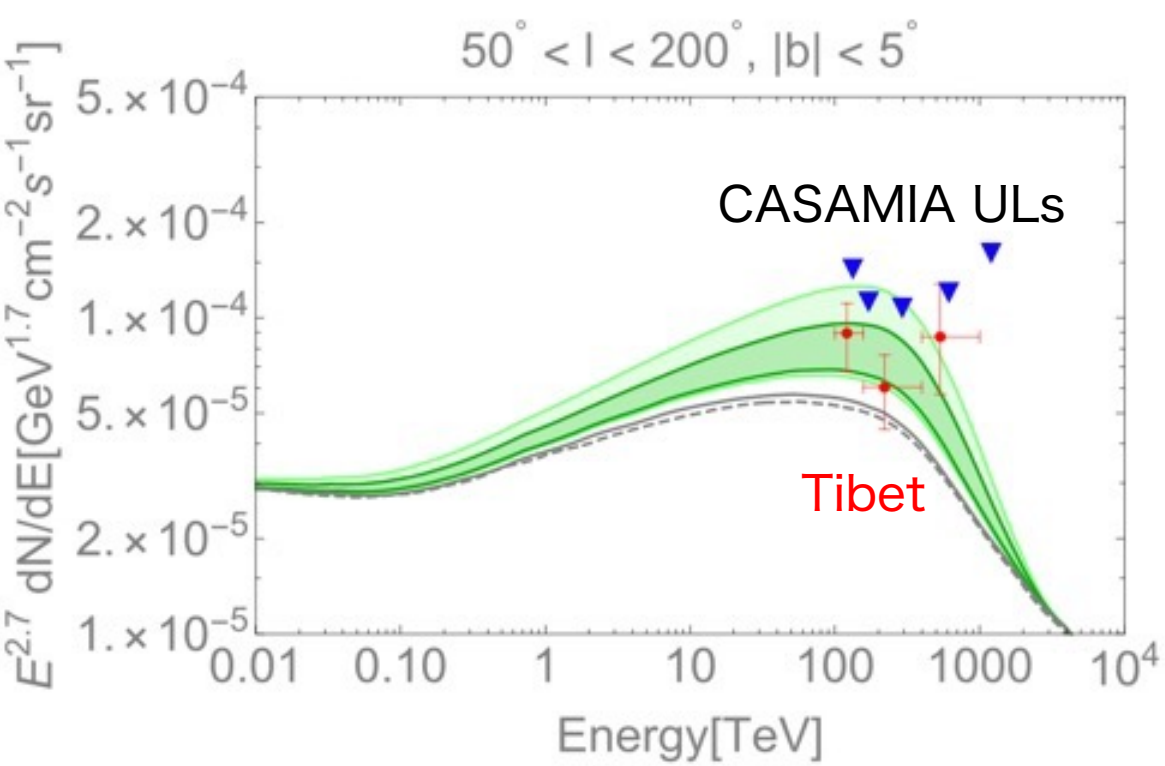

Black: True GDE model

Green: True GDE model + Unresolved Sources model

See also,
Riu & Wang, ApJL 914, L7 (2021)
Yan et al., Nat. Astron. 8, 628 (2024)

Source Contamination of Tibet GDE?

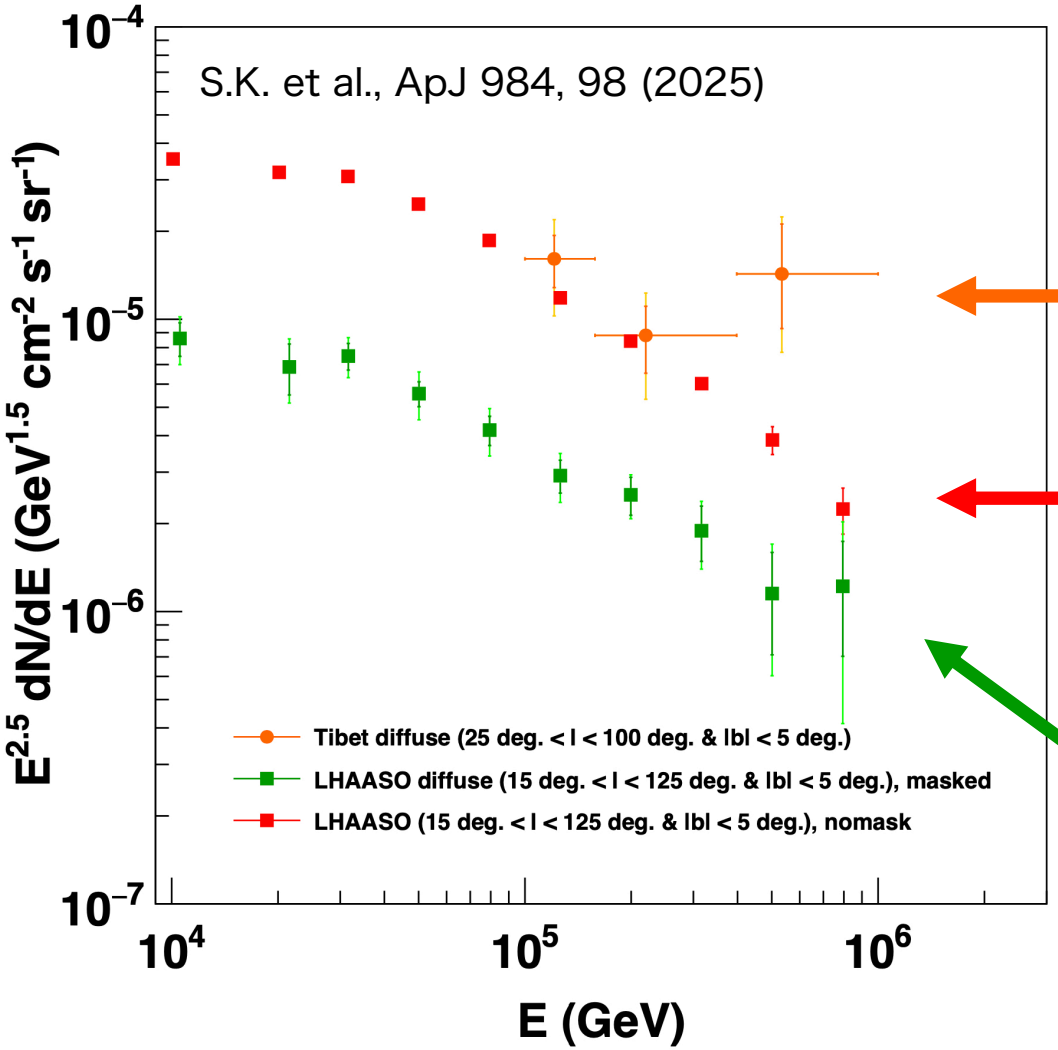

Tibet masked GDE flux (25° < l < 100° & |b| < 5°)

Amenomori et al., PRL, 126, 141101, 2021

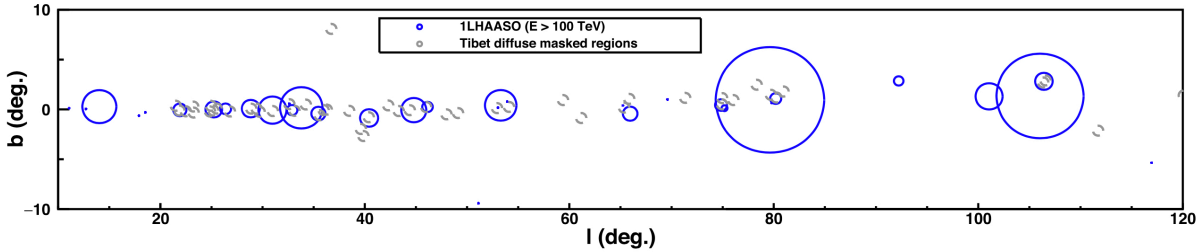

Not-masked LHAASO flux (15° < l < 125° & |b| < 5°)

Cao et al., PRL 134 081002, 2025

LHAASO masked GDE flux (15° < l < 125° & |b| < 5°)

Cao et al., PRL 134 081002, 2025

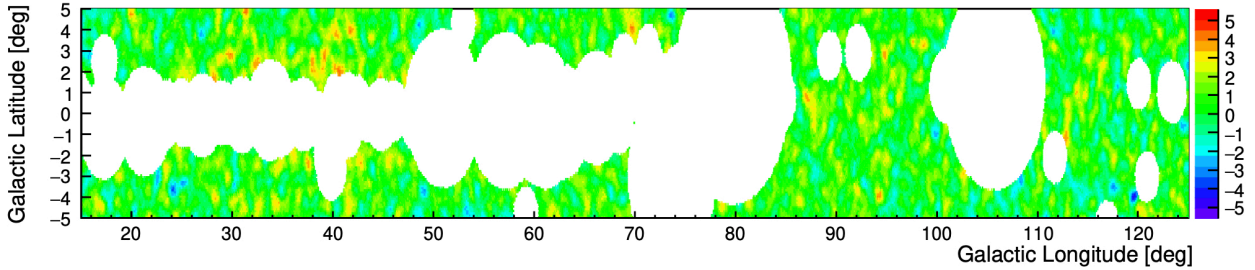

- ✓ ~5 times difference in Tibet GDE & LHAASO GDE (masked) @ >100TeV
- ✓ Tibet GDE & Not-masked LHAASO flux are consistent
- ✓ Tibet GDE is contaminated by γ-ray sources?

Source Contamination of Tibet GDE?

GDE: Galactic diffuse (γ-ray) emission

1st LHAASO catalog (2024) helps us to study the origin of Tibet GDE

LHAASO (×15 Tibet ASγ)

43 1LHAASO sources @ E >100TeV (2024)

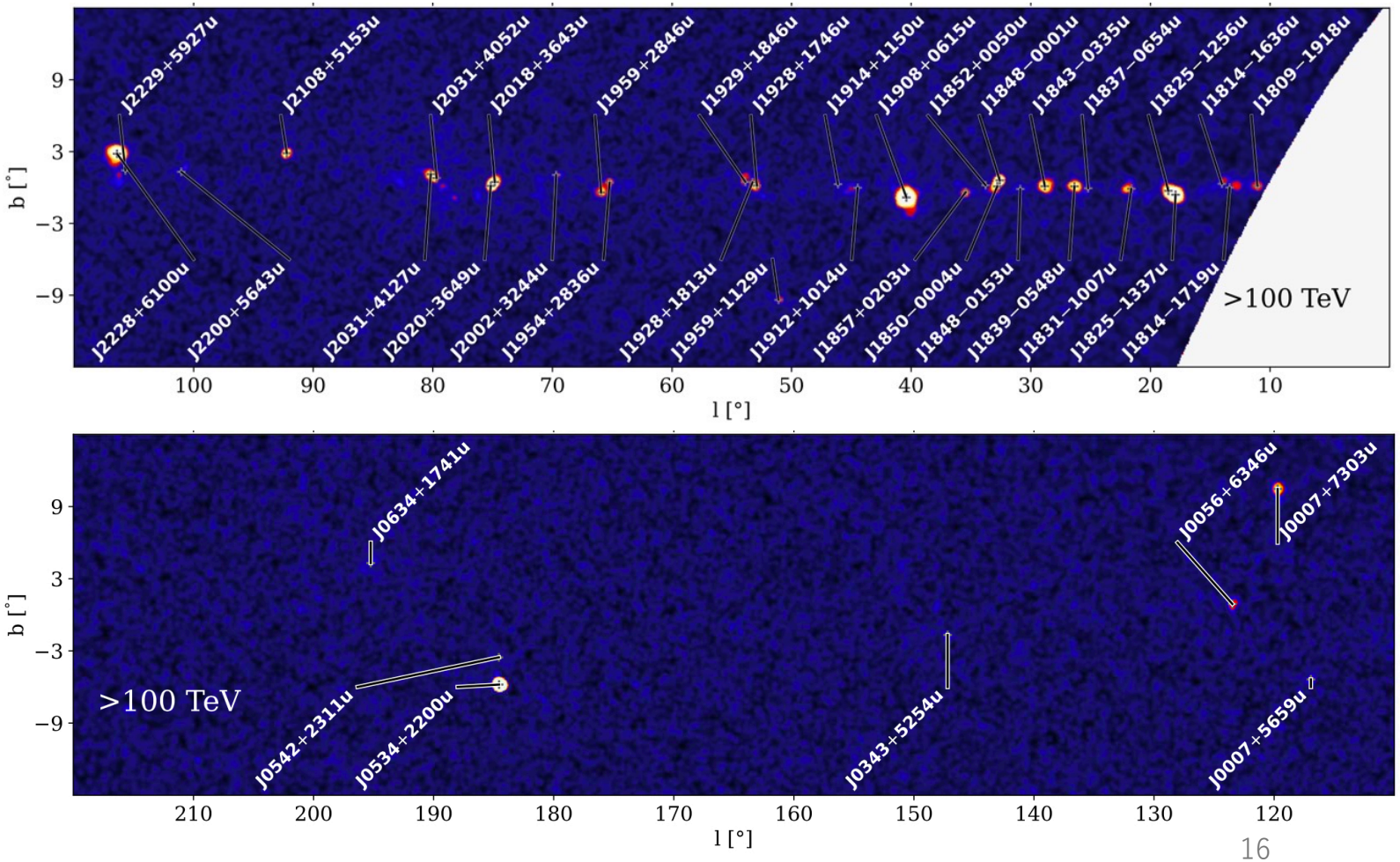

Cao et al., ApJS 271, 25 (2024)

Source Masking in the Tibet GDE Analysis in 2021

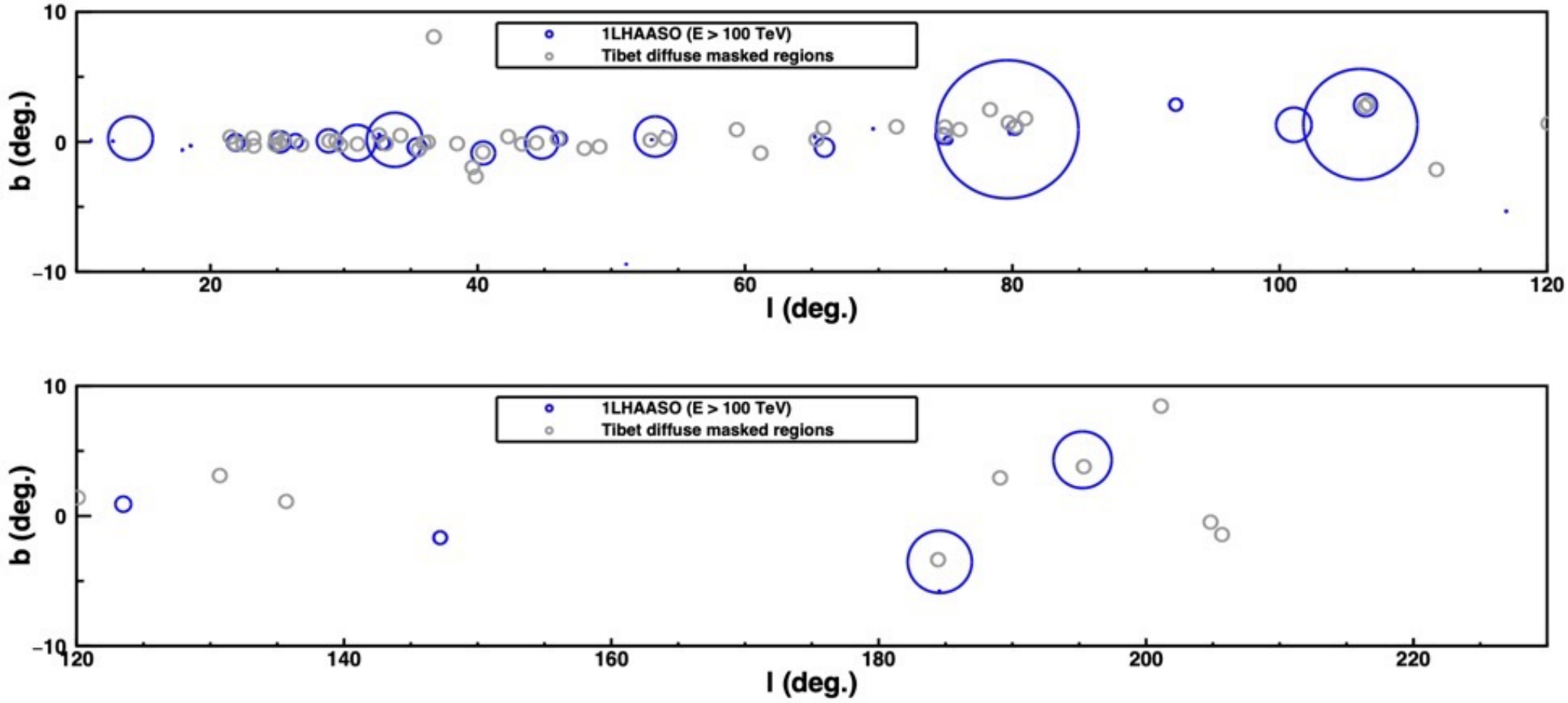

1st LHAASO catalog sources (detected @ > 10^{14} eV, 95% containment extension)
Tibet source masking (r = 0.5°) for TeVCat sources as of 2021

Tibet masking regions should be properly accounted for
to estimate the source contamination of Tibet GDE

Estimate of the Source Contamination

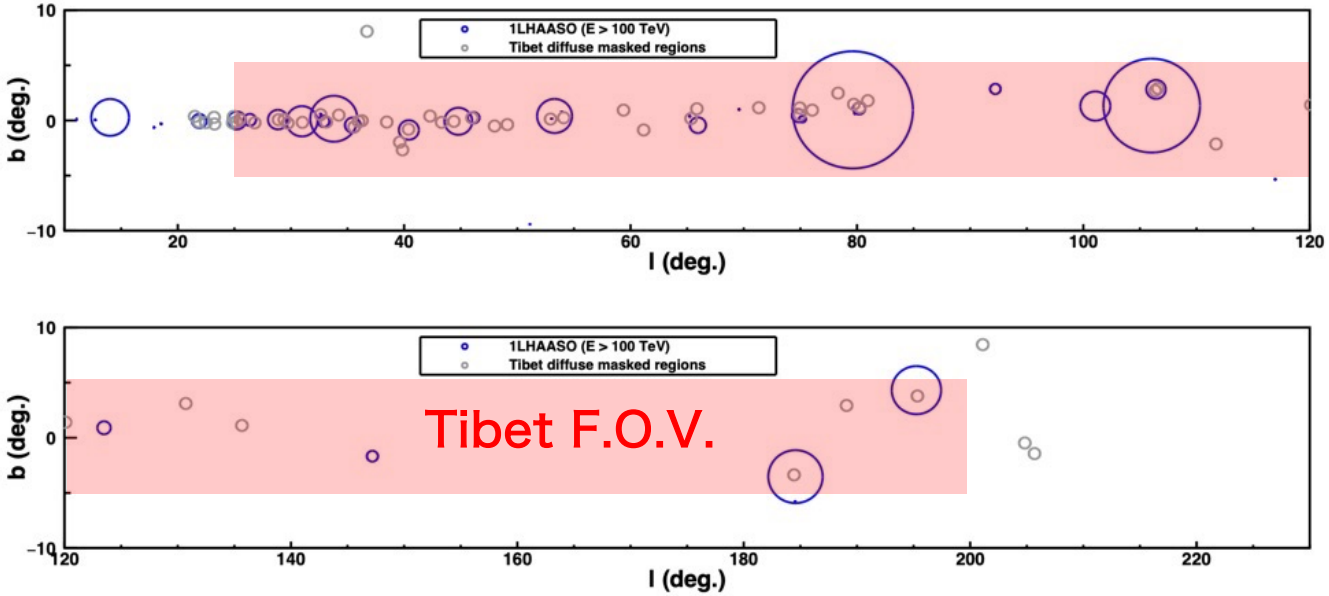

Source contamination is estimated as

$$F_{\mathrm{src,tot}}(E) = \sum_i \alpha_i N_{0,i} \left(\frac{E}{50\ \mathrm{TeV}} \right)^{-\Gamma_i}$$

$$\alpha_i = \left(N_{\mathrm{MC,tot}} - N_{\mathrm{MC,masked}} \right) / N_{\mathrm{MC,tot}}$$

N_0 & Γ: Best-fit PL parameters to KM2A data (@ E > 25 TeV)

Sum: over the sources detected @ E > 100TeV

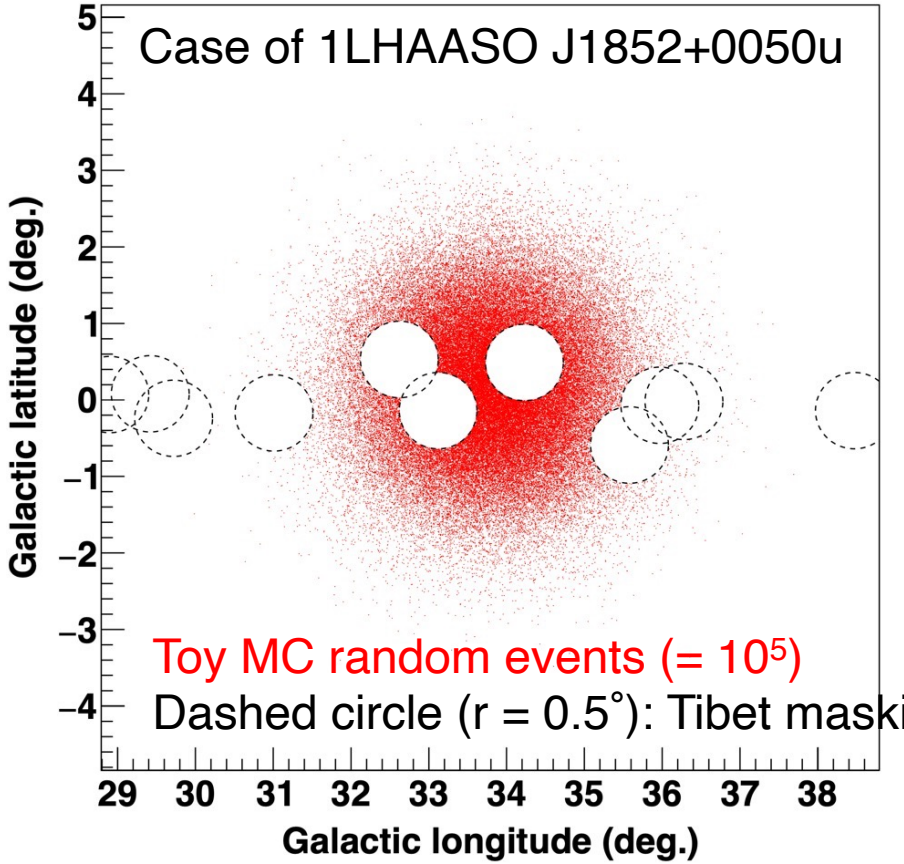

MC event generation from Gauss.$(\boldsymbol{x}_{\mathrm{src}}, \sigma^2)$

$$\sigma^2 = \sqrt{\sigma_{\mathrm{src}}^2 + \sigma_{\mathrm{tibet}}^2},$$

σ_{src}: 39% source extension

$\sigma_{\mathrm{tibet}} = 0.2°$: 39% PSF radius of Tibet (@ E>100TeV)

Source Contribution to the Tibet GDE Flux

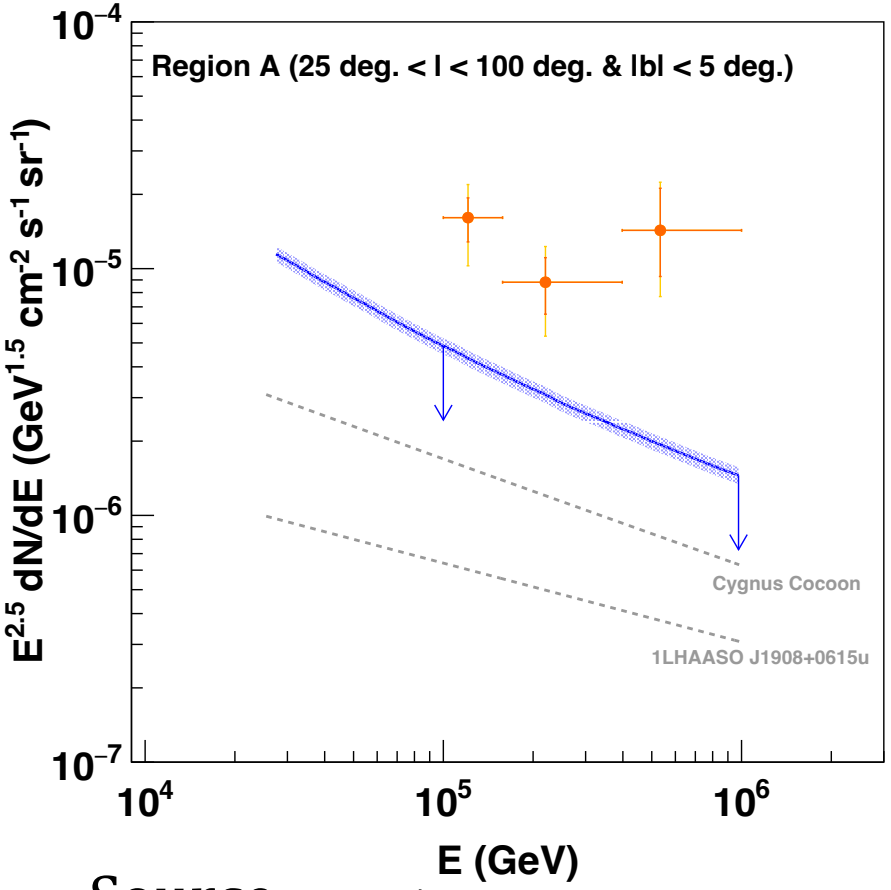

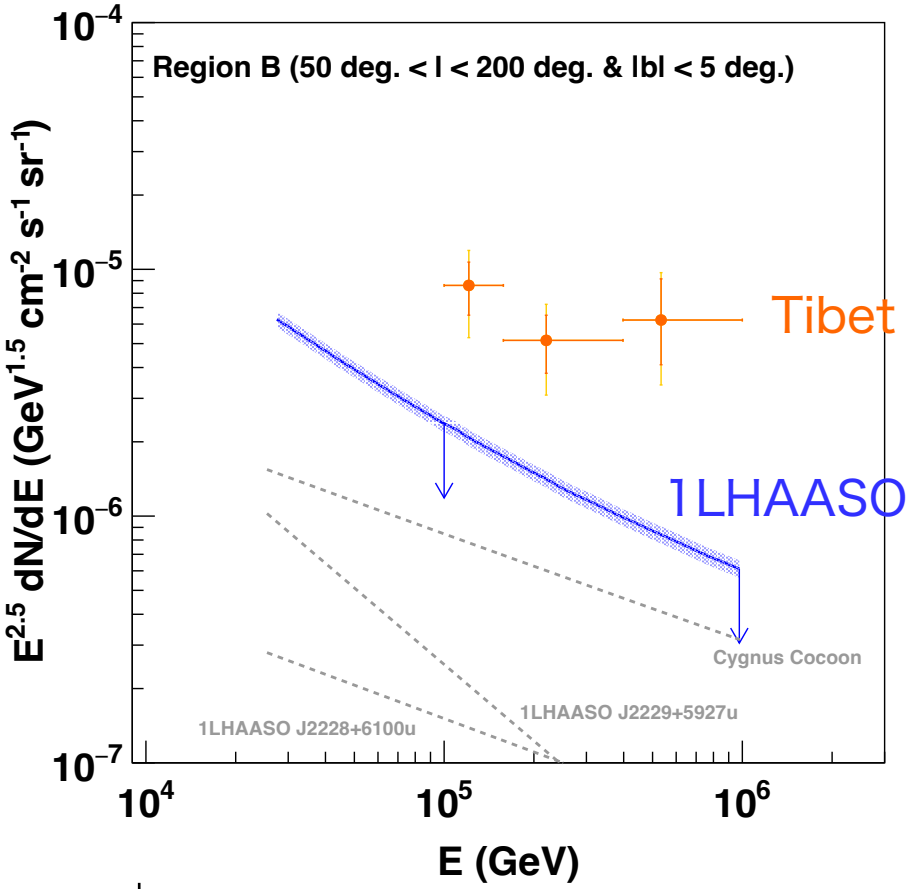

S.K. et al., ApJL 977, L3 (2024)

Tibet GDE flux (stat. & syst.)

1LHAASO(>100TeV)+Cygnus Cocoon

Source / Tibet GDE	Region A (25°<l<100° & |b|<5°)	Region B (50°<l<200° & |b|<5°)
121 TeV	< 26.9%±9.9%	< 24.1%±9.5%
220 TeV	< 34.8%±14.0%	< 27.4%±11.1%
534 TeV	$< 13.5\%^{+6.3\%}_{-7.7\%}$	$< 13.5\%^{+6.2\%}_{-7.6\%}$

Source contribution is subdominant

Tibet GDE @ E > 398TeV & 1stLHAASO Sources @ E >100TeV

S.K. et al., ApJL 961, L13 (2024)

No overlap b/w Tibet GDE events & sub-PeV LHAASO sources

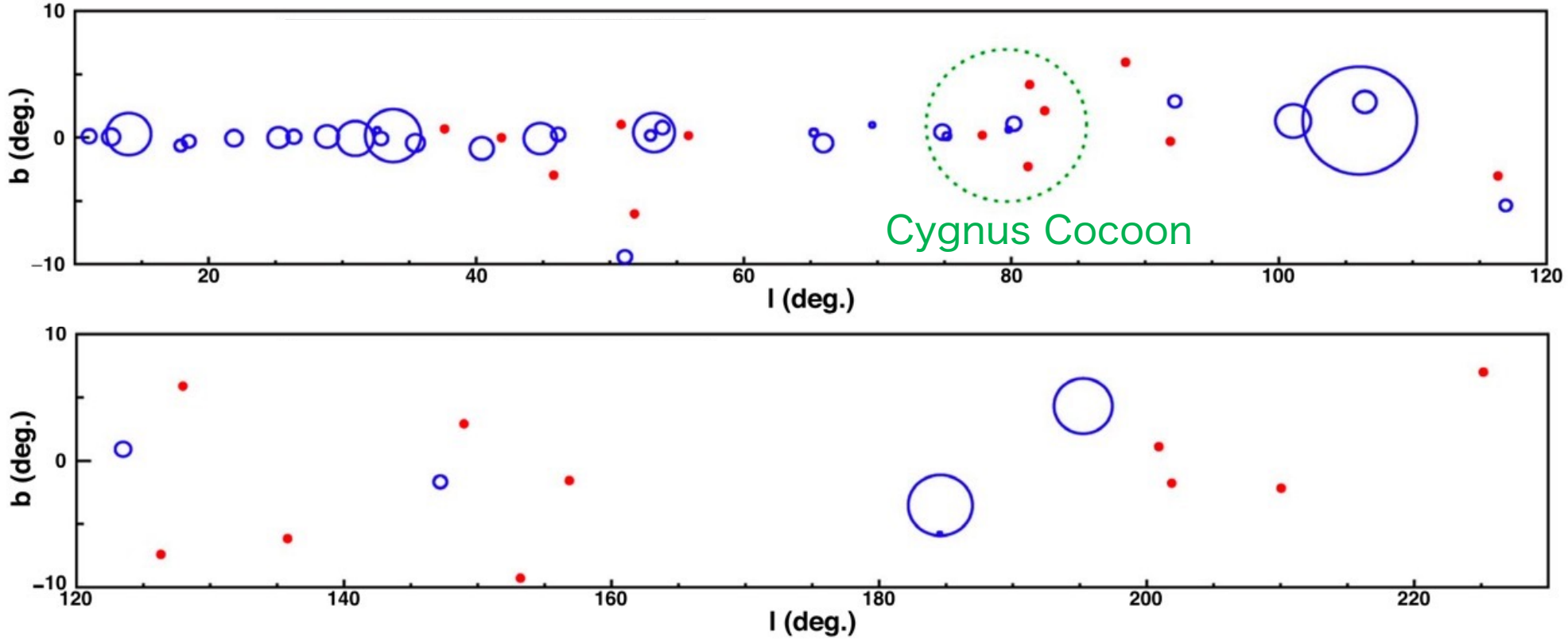

Tibet GDE events (E > 398TeV, 23 events)

1LHAASO sources @ > 100TeV (95% containment extension, 43 sources)

The 23 Tibet GDE events @ E > 398 TeV, except for 4 events from Cygnus, are likely of diffusive nature

Consistency with the LHAASO Measurements

S.K. et al., ApJL 977, L3 (2024)

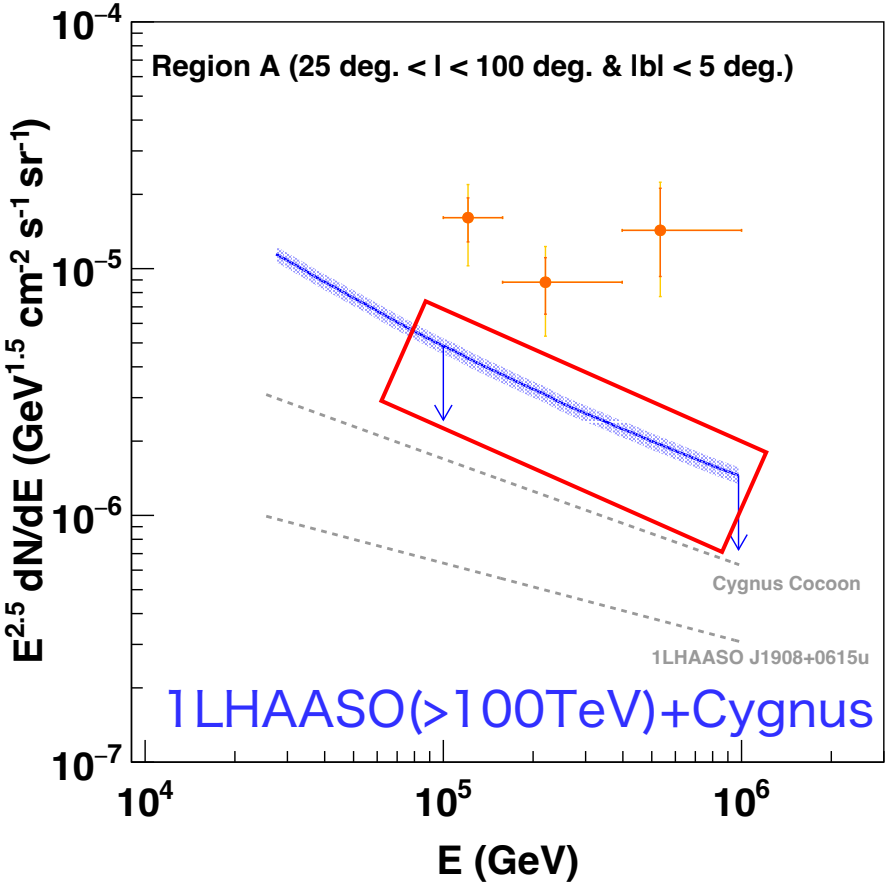

1LHAASO(>100TeV)+Cygnus Cocoon

+

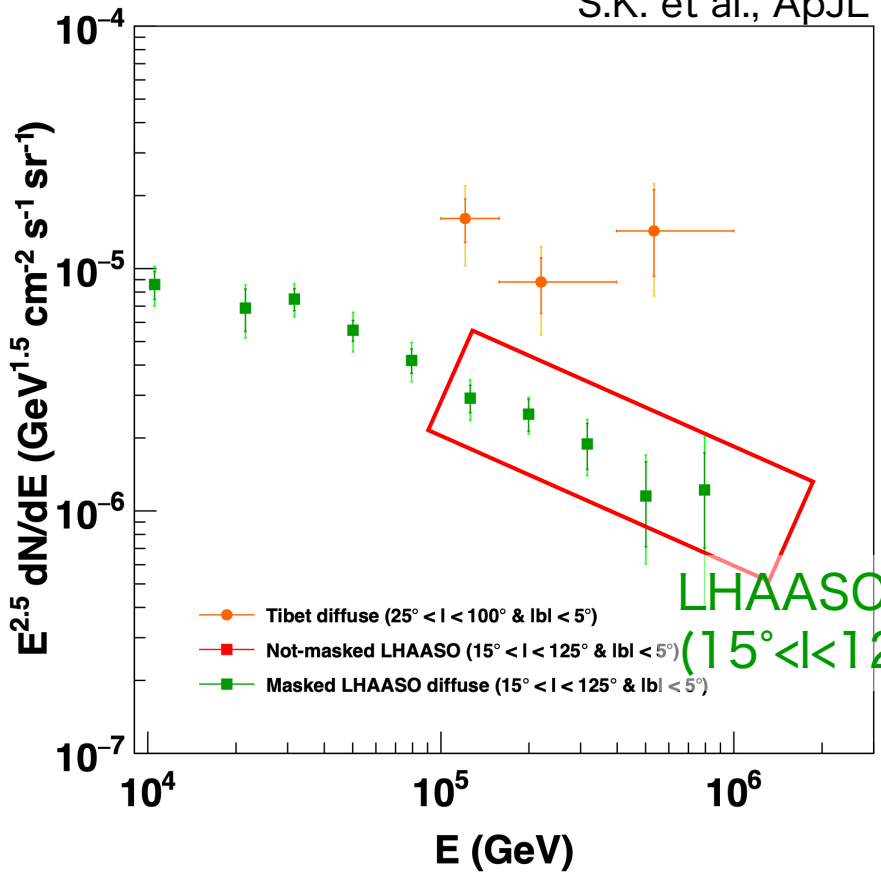

LHAASO GDE
(15°<l<125° & |b|<5°)

(Src + LHAASO GDE)/Tibet GDE	Region A (25°<l<100° & |b|<5°)
121 TeV	< 49.4%
220 TeV	< 65.5%
534 TeV	< 25.8%

Source contamination cannot account for the difference b/w Tibet & LHAASO GDE fluxes

Nature of the Tibet GDE Flux

S.K. et al., ApJL 977, L3 (2024)

GDE in Region A (25° < l < 100° & |b| < 5°)

Amenomori+., PRL 126, 141101 (2021)

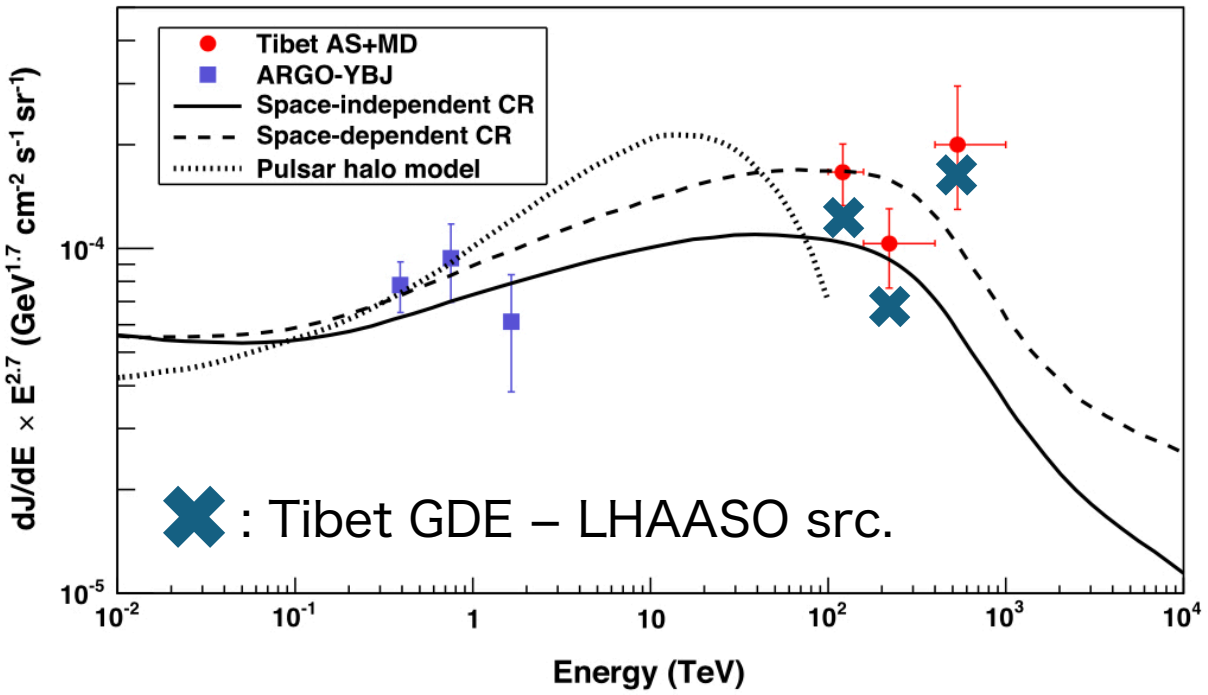

GDE in Region B (50° < l < 200° & |b| < 5°)

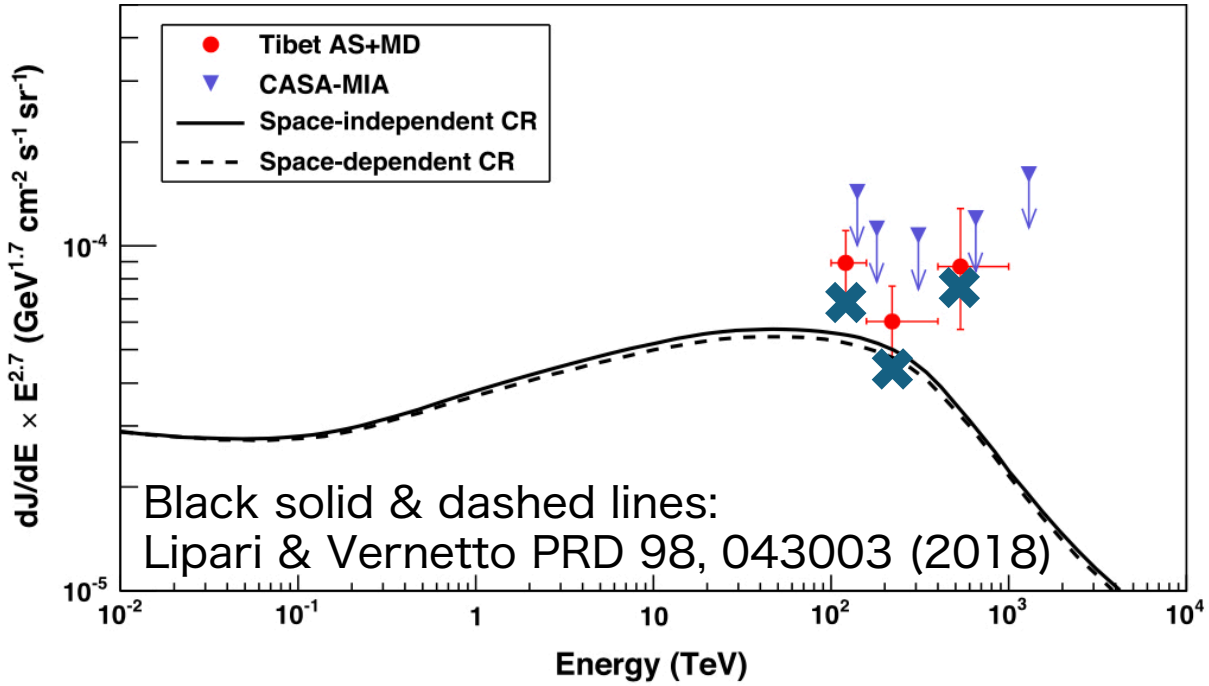

(Tibet GDE – Source) is (still) consistent w/ the GDE model of Lipari & Vernetto

Supporting the diffusive origin of Tibet GDE

※ Significant contribution from unresolved hadronic sources cannot be ruled out

Nature of the Tibet GDE Flux

S.K. et al., ApJL 977, L3 (2024)

Estimation of unresolved Leptonic contribution[1]

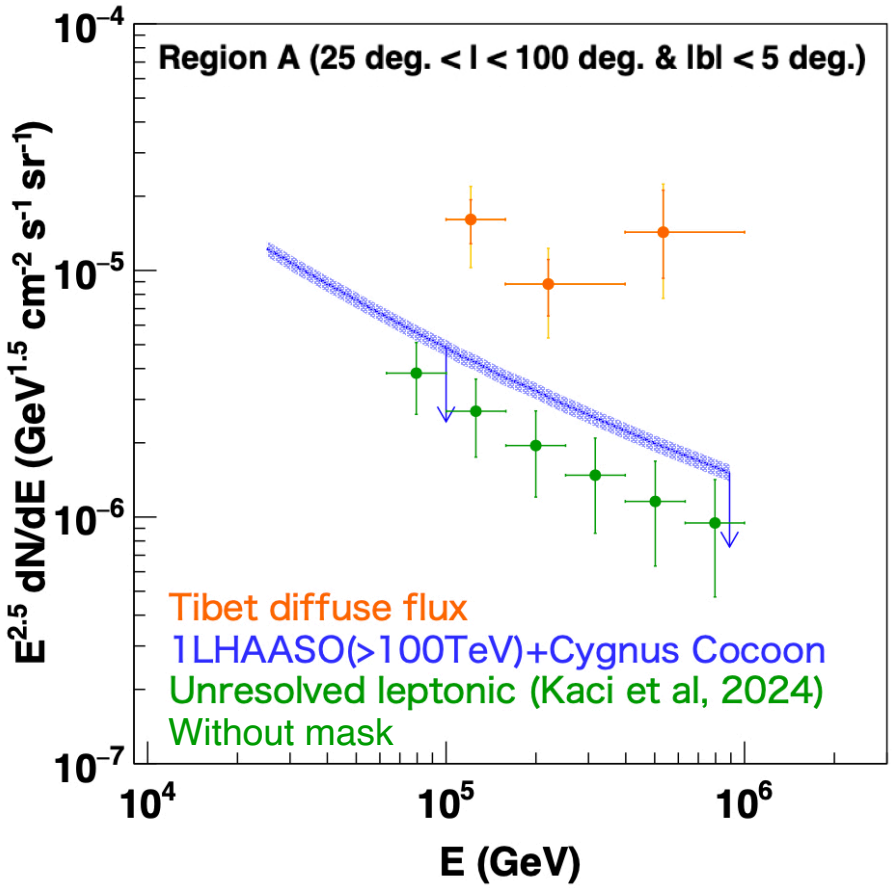

IceCube Galactic ν & Tibet GDE[2]

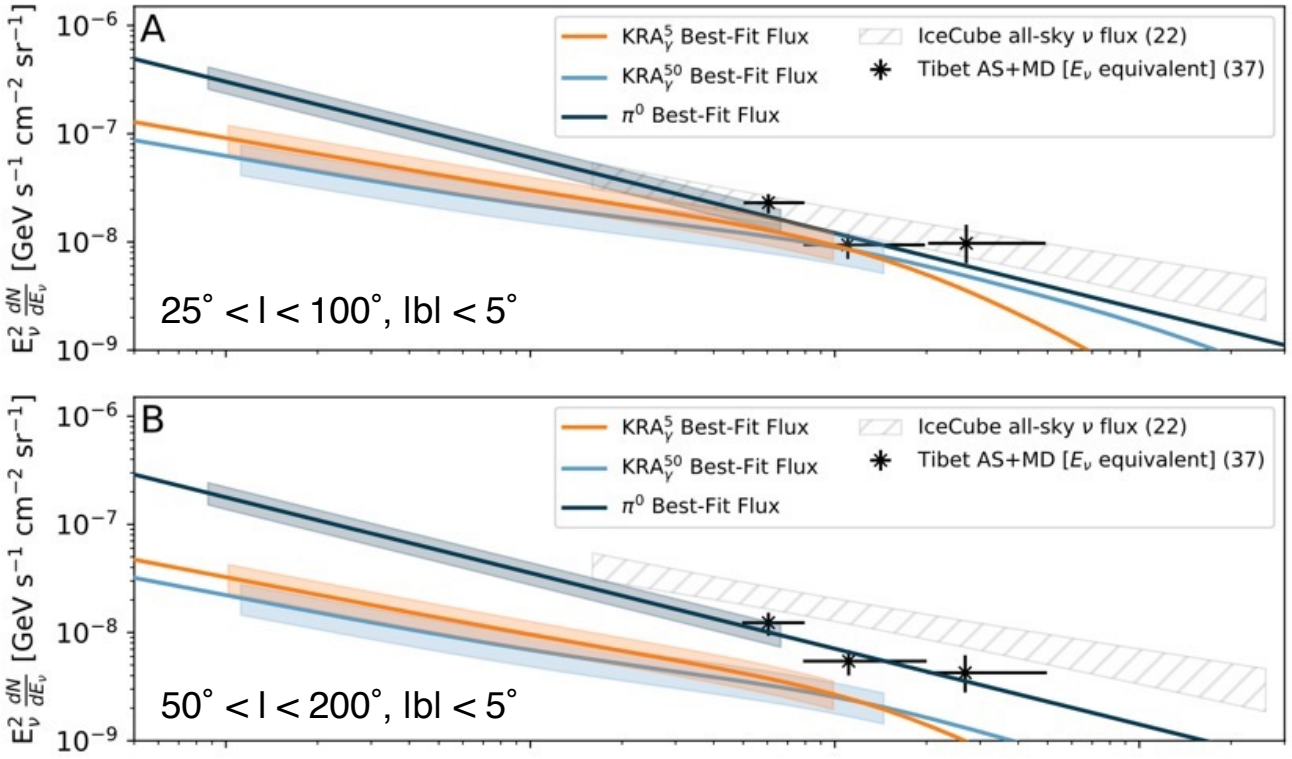

Consistent w/ IceCube ν flux (π^0 model)

Unresolved leptonic contribution should be $\lesssim$ 20%

Supporting the hadronic origin of Tibet GDE

1. Kaci et al., ApJL 975, L6 (2024)
2. IceCube Collaboration, Science 380, 1338 (2023)

Consistency with the LHAASO Measurements

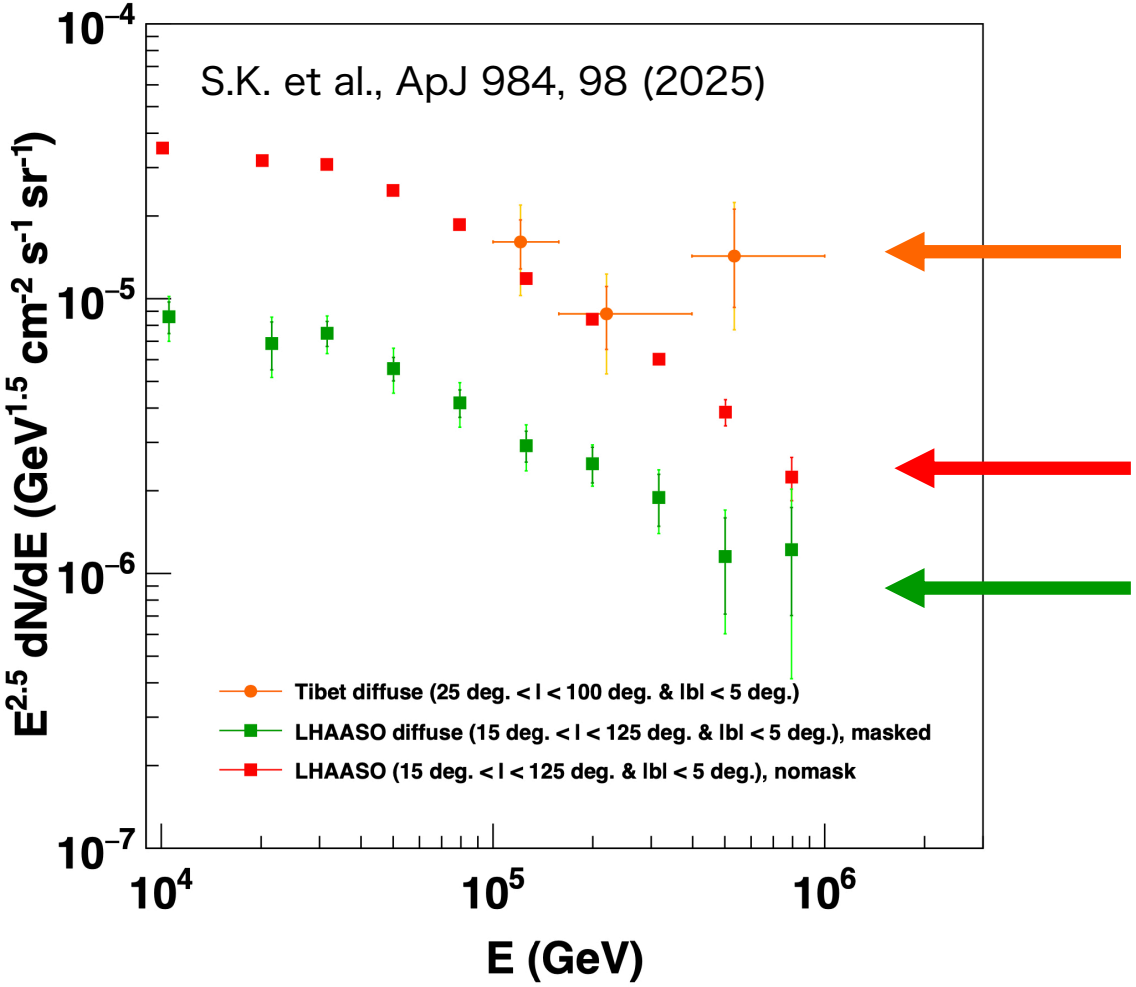

Tibet masked GDE flux (25° < l < 100° & |b| < 5°)

Amenomori et al., PRL, 126, 141101, 2021

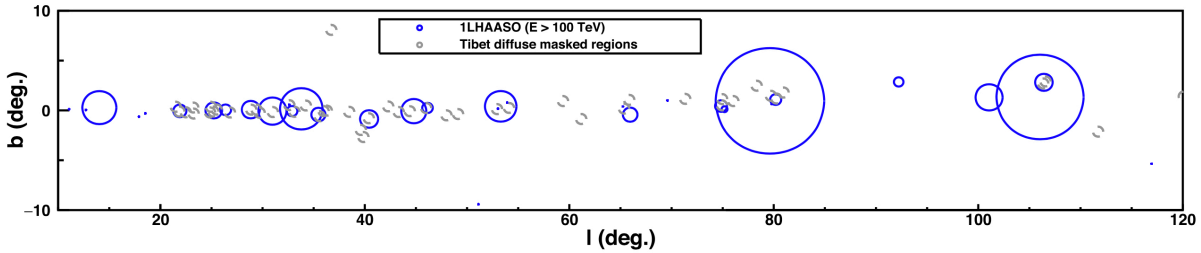

Not-masked LHAASO flux (15° < l < 125° & |b| < 5°)

Cao et al., PRL 134 081002, 2025

LHAASO masked GDE flux (15° < l < 125° & |b| < 5°)

Cao et al., PRL 134 081002, 2025

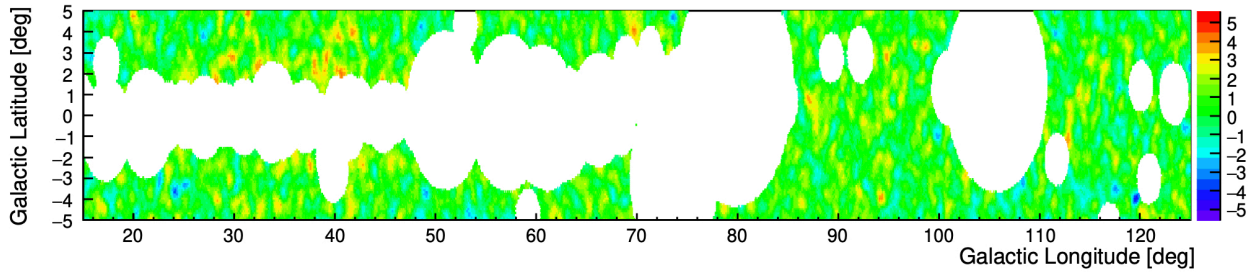

- ✓ Tibet GDE & Not-masked LHAASO flux are consistent
- ✓ Now we see Tibet GDE is dominated by hadronic diffuse γ rays

Sub-PeV Galactic γ-ray emission is likely dominated by hadronic GDE.
Difference in Tibet & LHAASO likely comes from different masking schemes.

Consistency with the LHAASO Measurements

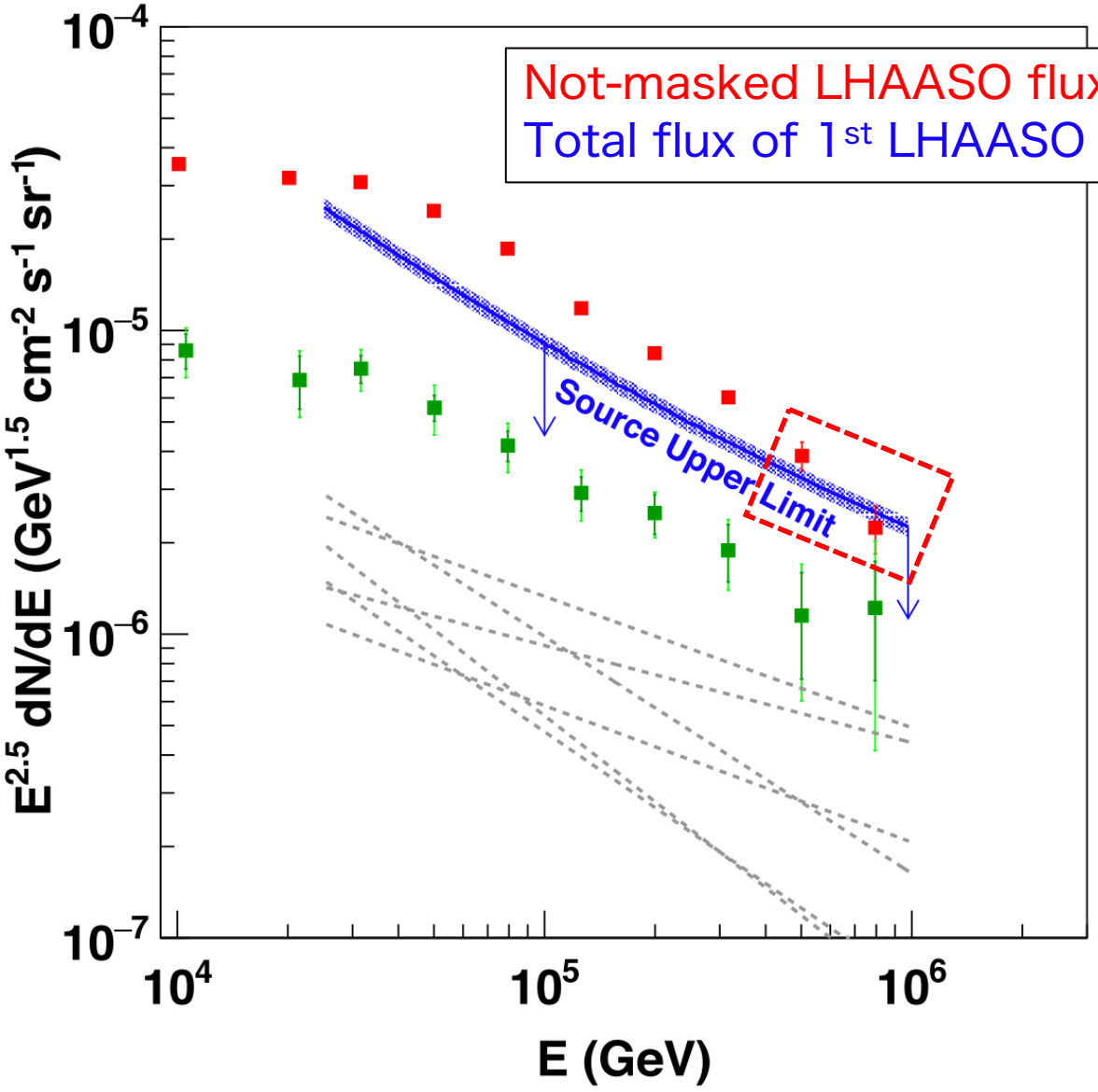

If simple PL spectra are assumed for all sources, the source flux dominates @ E > 500 TeV.

It is at odds w/ the fact that none of Tibet GDE events (E > 400TeV) overlap with these sources.

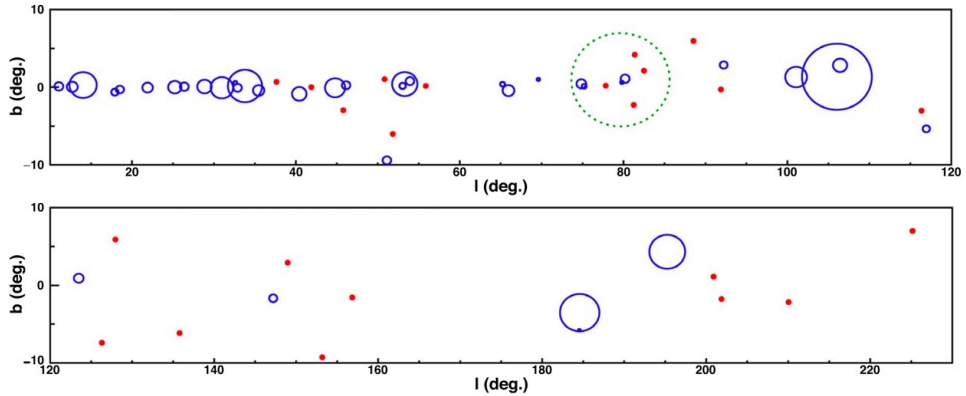

=> Many of the sources would have a cutoff in their spectra

Energy Spectra of Individual 1st LHAASO Catalog Sources

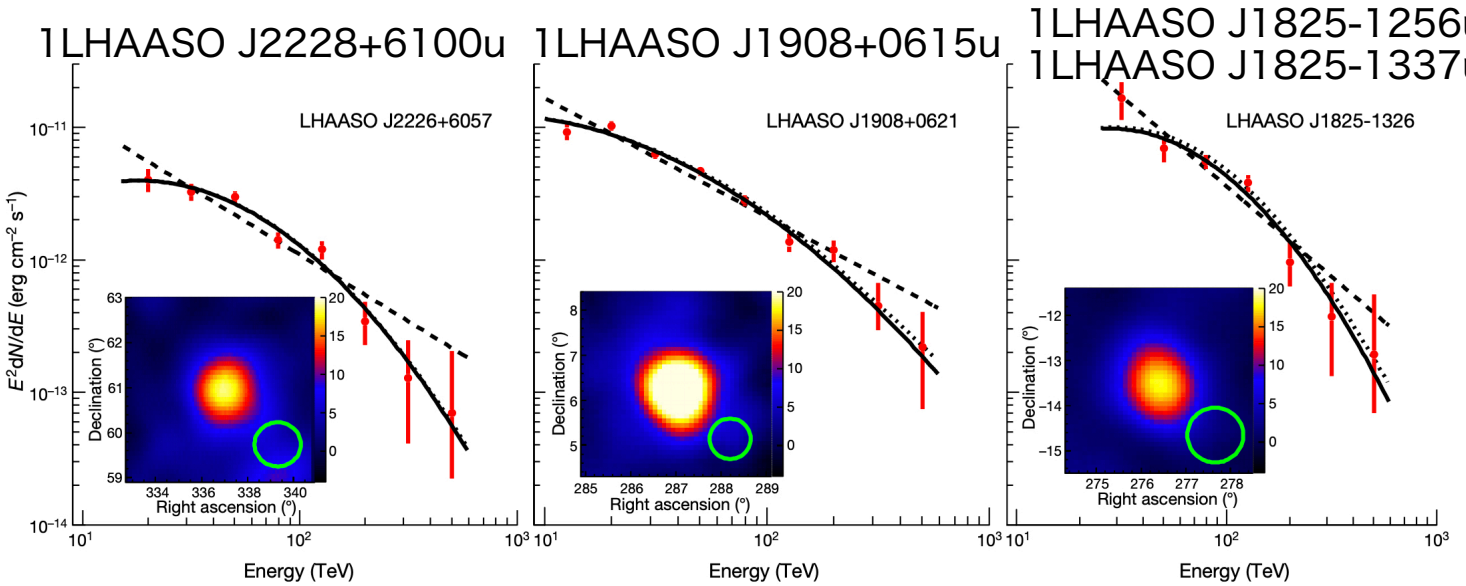

Cao et al., Nature 594, 33 (2021)

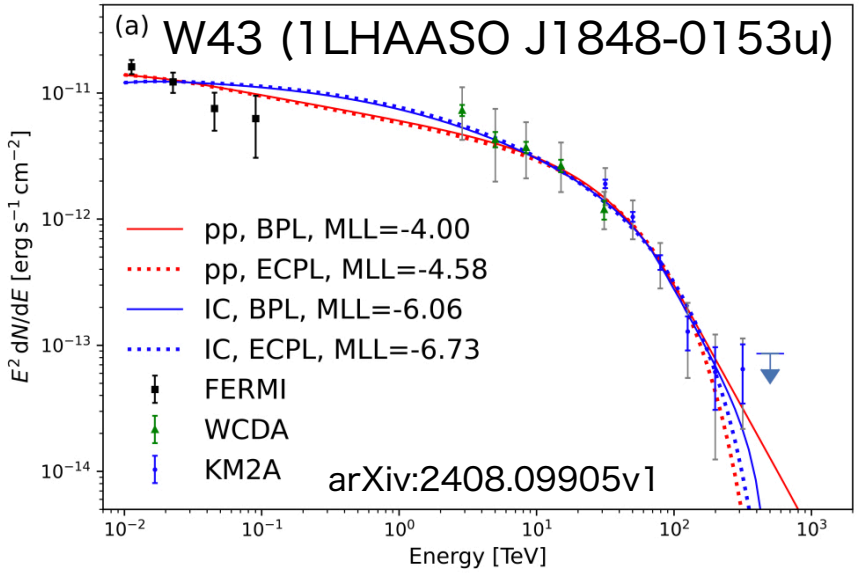

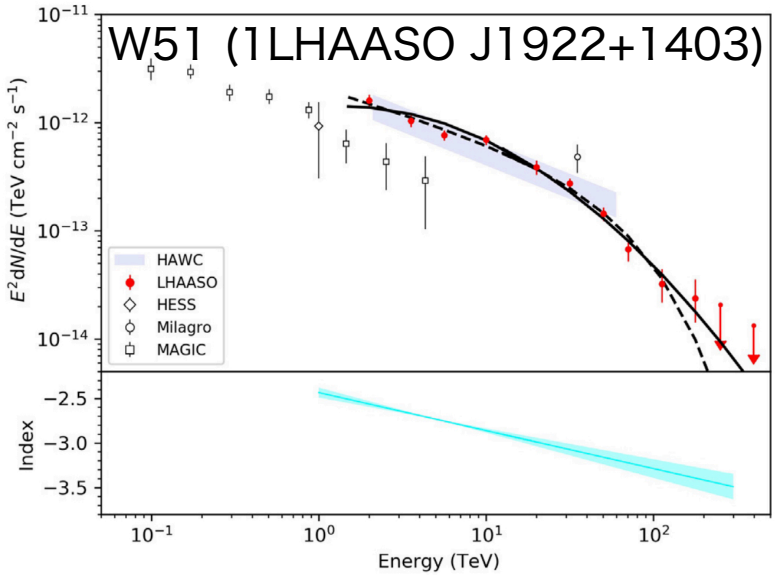

LHAASO Collaboration, Science Bulletin 69, 2833 (2024)

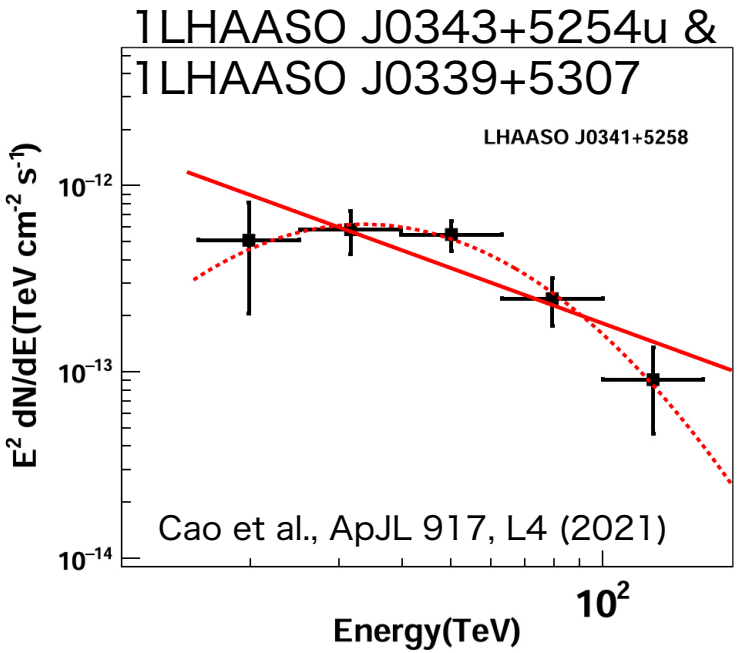

Many gamma-ray sources have a spectral break @ O(10TeV)

Spectral studies of more sources needed

An Implication from Our Results: Cygnus Super Bubble

LHAASO Collaboration, Science Bulletin 69, 449 (2024)

γ-ray significance maps (E >100TeV)

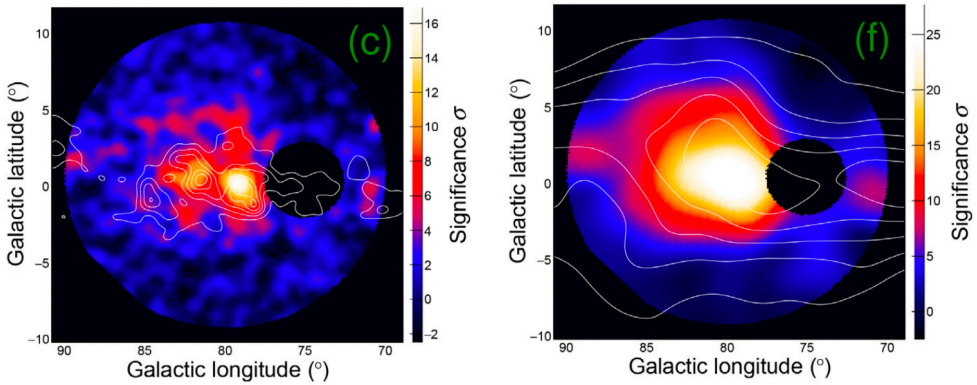

Longitude distribution (E >100TeV)

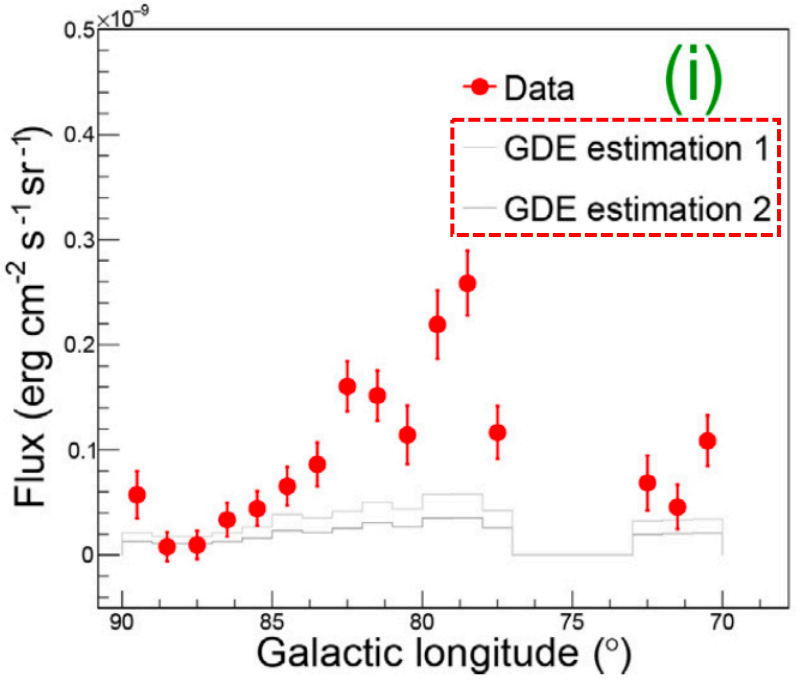

γ-ray energy spectrum

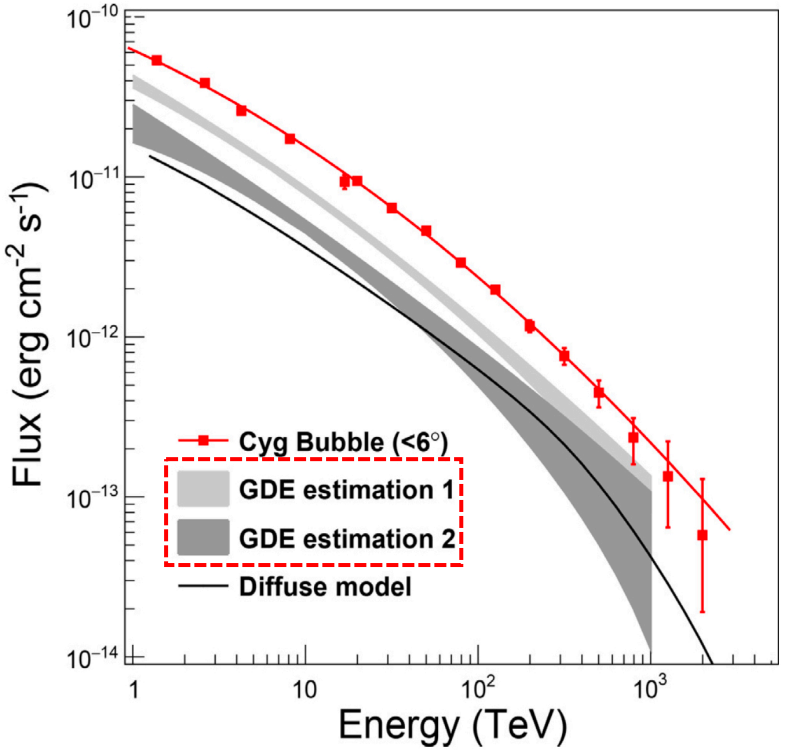

Estimate of GDE contamination based on the masked LHAASO GDE flux

=> Higher GDE contamination than previously thought ??

Summary

From the γ-ray observation by Tibet ASγ, we found

1. Astrophysical sub-PeV γ rays (Crab Nebula)
2. Promising PeVatron candidates (e.g., SNR G106.3+2.7)
3. Evidence for Galactic PeVatrons (Galactic diffuse)

Regarding the GDE flux @ E > 100 TeV measured by Tibet,

1. Contribution from resolved γ-ray sources is subdominant
2. Sub-PeV Galactic γ-ray emission is likely dominated by hadronic GDE
4. However, a significant contribution from yet-unresolved sources cannot be ruled out. Spectral measurement of individual sources is also important

Backup Slides

Estimation of Energy & Direction

2nd particle density

↓

γ-ray energy

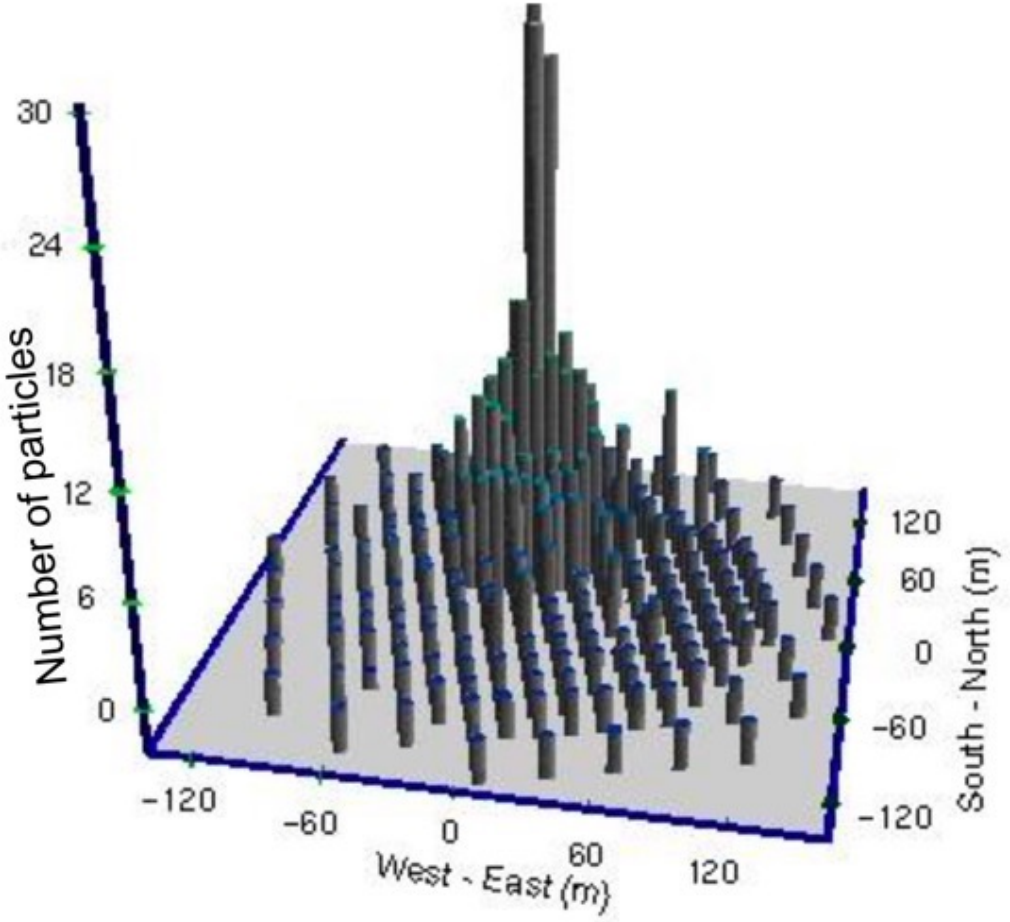

2nd particle timing

↓

γ-ray direction

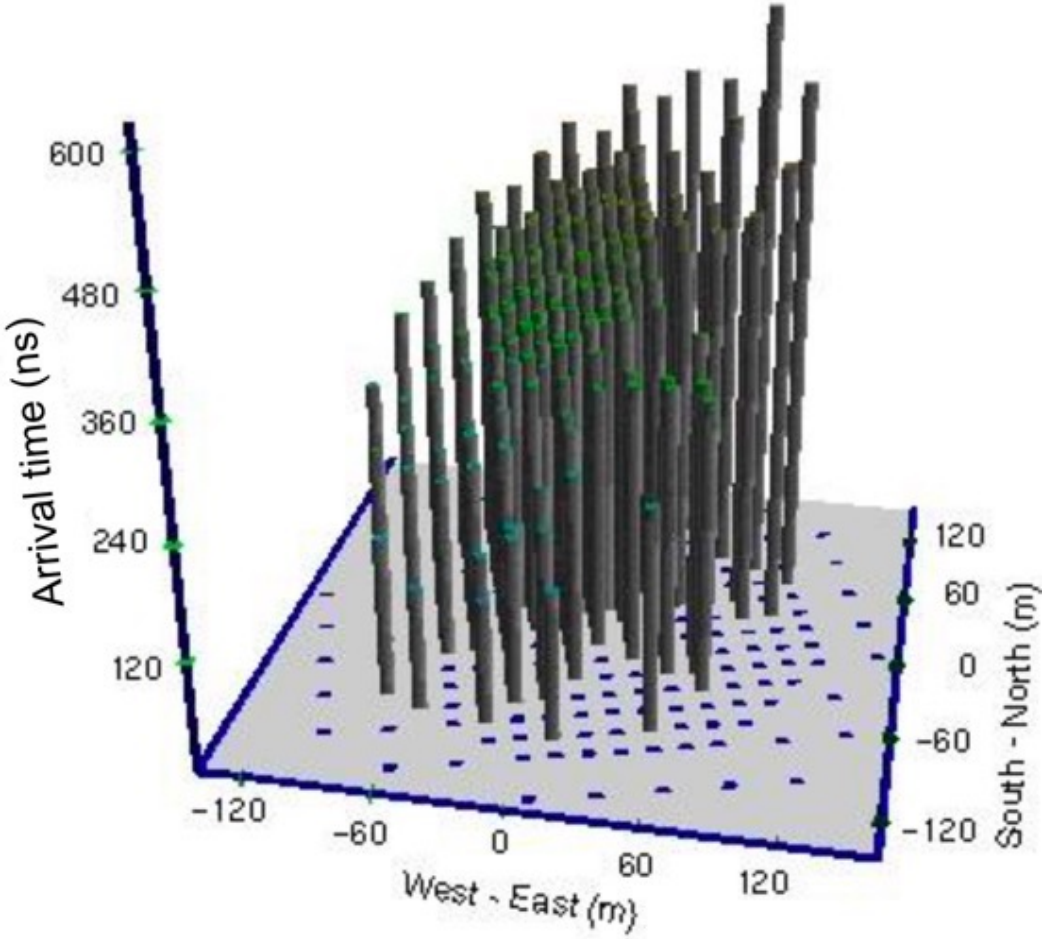

Tibet PSF Radius

From SM of Amenomori et al., PRL 126, 141101 (2021)

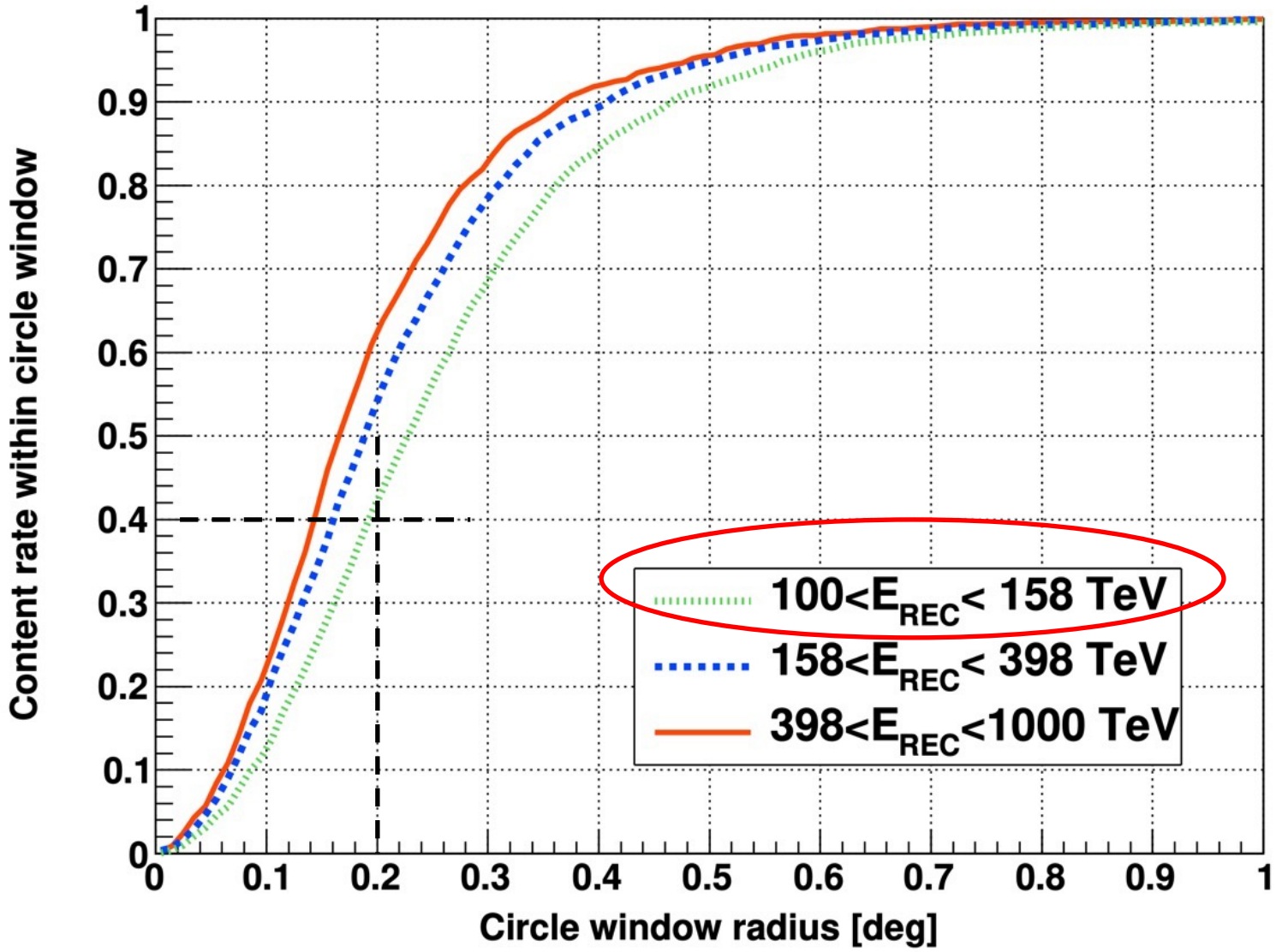

BG Rejection w/ an Underground Muon Detector Array

BGCR/Src γ > 10^2 @ sub-PeV

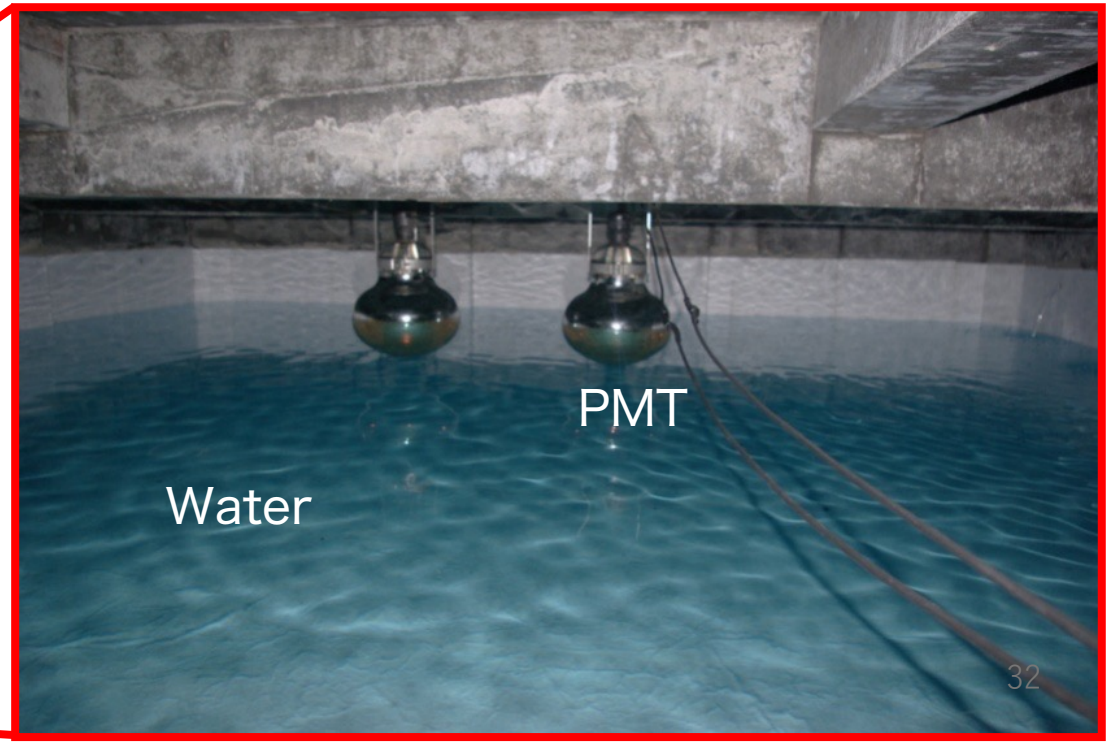

Crab Nebula: Spillover

Amenomori et al., PRL 123, 051105 (2019)

improved at higher energies. The energy bin purities evaluated from the smearing by the energy resolution is estimated to be 83% (86%) for $100 < E \leq 250$ TeV ($250 < E \leq 630$ TeV). In each bin, the spillover fractions from lower and higher energy bins are 14% (12%) and 3% (2%), respectively, for $100 < E \leq 250$ TeV ($250 < E \leq 630$ TeV).

Estimation:

In 100 TeV < E < 250 TeV (20 events):

Spillover from E < 100 TeV: 20 * 0.14 = 2.8 events

Spillover from E > 250 TeV: 20 * 0.03 = 0.6 events

In 250 TeV < E < 630 TeV (4 events):

Spillover from E < 250 TeV: 4 * 0.12 = 0.5 events

Spillover from E > 250 TeV: 4 * 0.02 = 0.1 events

Masked TeVCat Sources (2021)

S. K. et al., ApJL 977, L3 (2024)

Table 1
Sky Regions Masked in the Tibet Diffuse Analysis

l (deg)	b (deg)	Masked Source	References
120.10	1.41	Tycho	S. Archambault et al. (2017)
130.71	3.11	3C 58	J. Aleksić et al. (2014a)
135.67	1.12	LS I+61 303	J. Albert et al. (2006)
184.44	−3.36	HAWC J0543+233	The Astronomer's Telegram[a]
189.08	2.93	IC 443	V. A. Acciari et al. (2009a)
195.34	3.79	Geminga	A. A. Abdo et al. (2009)
205.68	−1.43	HESS J0632+057	H.E.S.S. collaboration (2018)
204.82	−0.47	HAWC J0635+070	The Astronomer's Telegram[b]
201.11	8.45	2HWC J0700+143	A. U. Abeysekara et al. (2017)
21.50	0.37	HESS J1828-099	H.E.S.S. collaboration (2018)
36.72	8.08	2HWC J1829+070	A. U. Abeysekara et al. (2017)
21.86	−0.12	HESS J1831-098	H.E.S.S. collaboration (2018)
23.21	0.29	HESS J1832-085	H.E.S.S. collaboration (2018)
22.48	−0.19	HESS J1832-093	H.E.S.S. collaboration (2018)
23.25	−0.32	HESS J1834-087	H.E.S.S. collaboration (2018)
24.94	0.36	MAGIC J1835-069	MAGIC Collaboration et al. (2018)
24.86	−0.21	MAGIC J1837-073	MAGIC Collaboration et al. (2018)
25.49	0.09	2HWC J1837-065	A. U. Abeysekara et al. (2017)
25.18	−0.12	HESS J1837-069	H.E.S.S. collaboration (2018)
26.80	−0.21	HESS J1841-055	H.E.S.S. collaboration (2018)
28.90	0.07	HESS J1843-033	H.E.S.S. collaboration (2018)
29.42	0.08	HESS J1844-030	H.E.S.S. collaboration (2018)
29.72	−0.24	HESS J1846-029	H.E.S.S. collaboration (2018)
31.01	−0.17	HESS J1848-018	H.E.S.S. collaboration (2018)
32.62	0.53	IGR J18490-0000	H.E.S.S. collaboration (2018)
34.23	0.49	2HWC J1852+013	A. U. Abeysekara et al. (2017)
33.12	−0.14	HESS J1852-000	H.E.S.S. collaboration (2018)
35.97	−0.07	HESS J1857+026	H.E.S.S. collaboration (2018)
36.28	−0.02	MAGIC J1857.6+0297	J. Aleksić et al. (2014b)
35.58	−0.59	HESS J1858+020	H.E.S.S. collaboration (2018)
38.47	−0.14	2HWC J1902+048	A. U. Abeysekara et al. (2017)
42.29	0.40	2HWC J1907+084	A. U. Abeysekara et al. (2017)
40.39	−0.79	MGRO J1908+06	F. Aharonian et al. (2009)
39.61	−1.96	SS 433 w1	A. U. Abeysekara et al. (2018b)
43.32	−0.17	W 49B	H.E.S.S. Collaboration et al. (2018)
44.40	−0.08	HESS J1912+101	H.E.S.S. collaboration (2018)
39.86	−2.67	SS 433 e1	A. U. Abeysekara et al. (2018b)
46.00	0.24	2HWC J1914+117	A. U. Abeysekara et al. (2017)
47.99	−0.50	2HWC J1921+131	A. U. Abeysekara et al. (2017)
49.12	−0.37	W 51	J. Aleksić et al. (2012)
52.93	0.13	2HWC J1928+177	A. U. Abeysekara et al. (2017)
54.10	0.25	SNR G054.1+00.3	V. A. Acciari et al. (2010)
59.38	0.94	2HWC J1938+238	A. U. Abeysekara et al. (2017)
61.16	−0.86	2HWC J1949+244	A. U. Abeysekara et al. (2017)
65.86	1.06	2HWC J1953+294	A. U. Abeysekara et al. (2017)
65.35	0.18	2HWC J1955+285	A. U. Abeysekara et al. (2017)
71.33	1.16	2HWC J2006+341	A. U. Abeysekara et al. (2017)
74.95	1.14	VER J2016+371	E. Aliu et al. (2014)
74.93	0.51	MGRO J2019+37	A. A. Abdo et al. (2012)
76.05	0.94	Milagro Diffuse	A. A. Abdo et al. (2008)
78.33	2.48	VER J2019+407	E. Aliu et al. (2013)
79.72	1.47	MGRO J2031+41	A. A. Abdo et al. (2012)
80.96	1.80	ARGO J2031+4157	B. Bartoli et al. (2014)
80.25	1.20	TeV J2032+4130	A. U. Abeysekara et al. (2018a)
106.35	2.71	SNR G106.3+02.7	V. A. Acciari et al. (2009b)
106.58	2.91	Boomerang	A. A. Abdo et al. (2009)
111.72	−2.13	Cassiopeia A	J. Albert et al. (2007)

Notes. Each of the masked regions has a fixed radius of 0.°5. The first and second columns show the center of the masked region in the Galactic longitude and latitude, respectively. The third column shows the masked gamma-ray source, which is registered in the TeVCat catalog. The fourth column gives the reference, which determines the coordinates of the masked source position presented in the TeVCat catalog.

[a] https://www.astronomerstelegram.org/?read=10941
[b] https://www.astronomerstelegram.org/?read=12013

Total ~ 60 sources

Contribution from the Cygnus Cocoon

S.K. et al., ApJL 977, L3 (2024)

Source	Components	α_{2000} (°)	δ_{2000} (°)	r_{39} (°)	TS	N_0 ($\mathrm{TeV^{-1}m^{-2}s^{-1}}$)	Γ
LHAASO J2027+4119	KM2A	307.43 ± 0.16	41.05 ± 0.13	2.17 ± 0.10	145	$(0.62 \pm 0.05) \times 10^{-15}$@50 TeV	-2.99 ± 0.07
	WCDA	306.90 ± 0.23	41.33 ± 0.16	2.28 ± 0.14	251	$(1.27 \pm 0.14) \times 10^{-9}$@7 TeV	-2.63 ± 0.08
HI	KM2A				108	$(0.69 \pm 0.10) \times 10^{-15}$@50 TeV	-2.94 ± 0.12
	WCDA				60	$(1.43 \pm 0.26) \times 10^{-9}$@7 TeV	-2.66 ± 0.12
MC	KM2A				88	$(0.46 \pm 0.06) \times 10^{-15}$@50 TeV	-2.87 ± 0.14
	WCDA				67	$(1.08 \pm 0.19) \times 10^{-9}$@7 TeV	-2.73 ± 0.13
LHAASO J2031+4057	WCDA	307.89 ± 0.09	40.96 ± 0.16	0.33 ± 0.08	115	$(0.11 \pm 0.06) \times 10^{-9}$@7 TeV	-2.75 ± 0.17

Table S1: The fitting results for the components of Cygnus Bubble.

Warning

WCDA Index vs KM2A Index

LHAASO カタログより、WCDA・KM2A両方で検出されたもののみ考慮

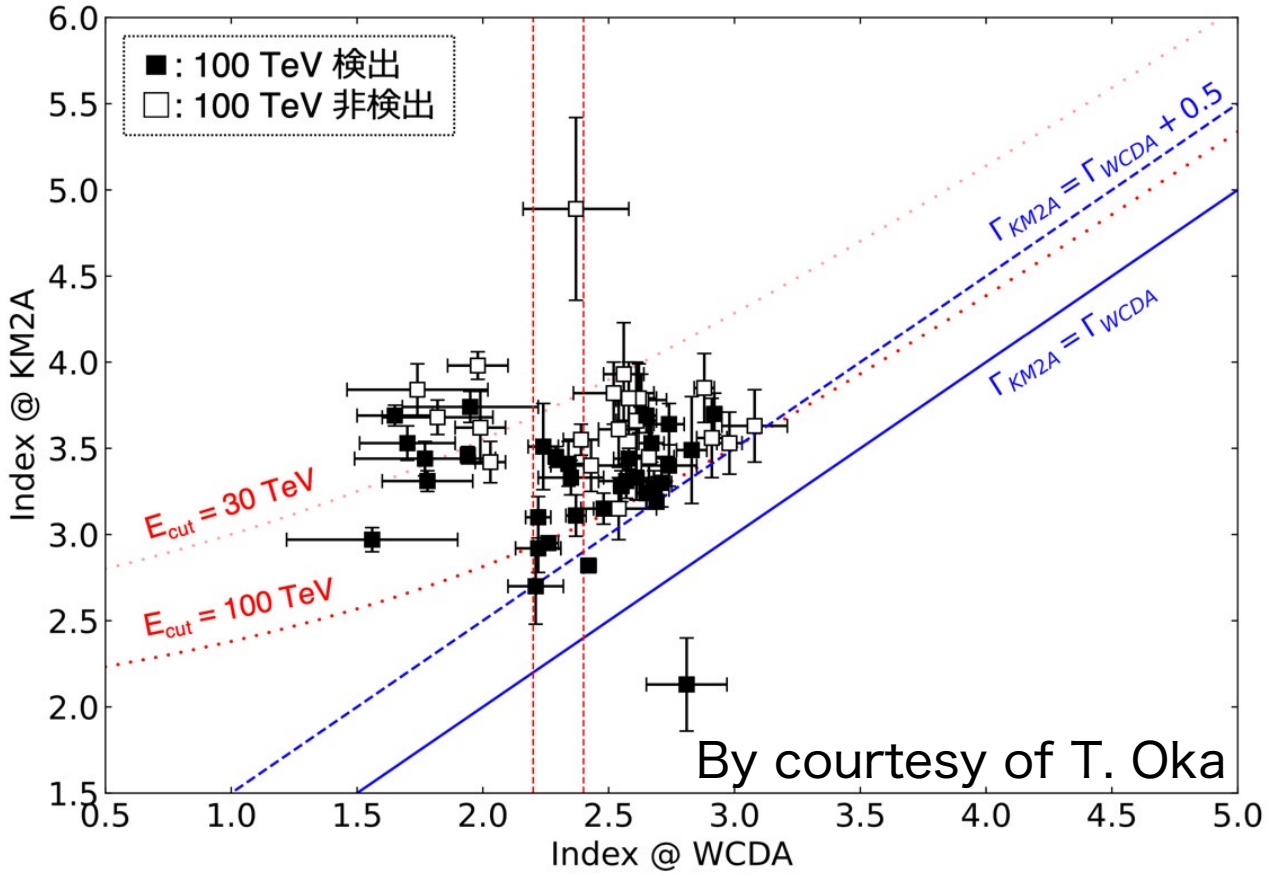

The flux is calculated based on the results given by KM2A @ E > 25TeV.
However, almost all spectra show the softening in the WCDA & KM2A observations.
Therefore, spectra @ E > 100 TeV would also soften from those @ 25TeV < E < 100TeV.
The estimated resolved source fraction @ E > 100 TeV should be considered as an upper limit

Is It Natural to Have No Overlap?

S.K. et al., ApJL 961, L13 (2024)

Expected # of accidental overlap:

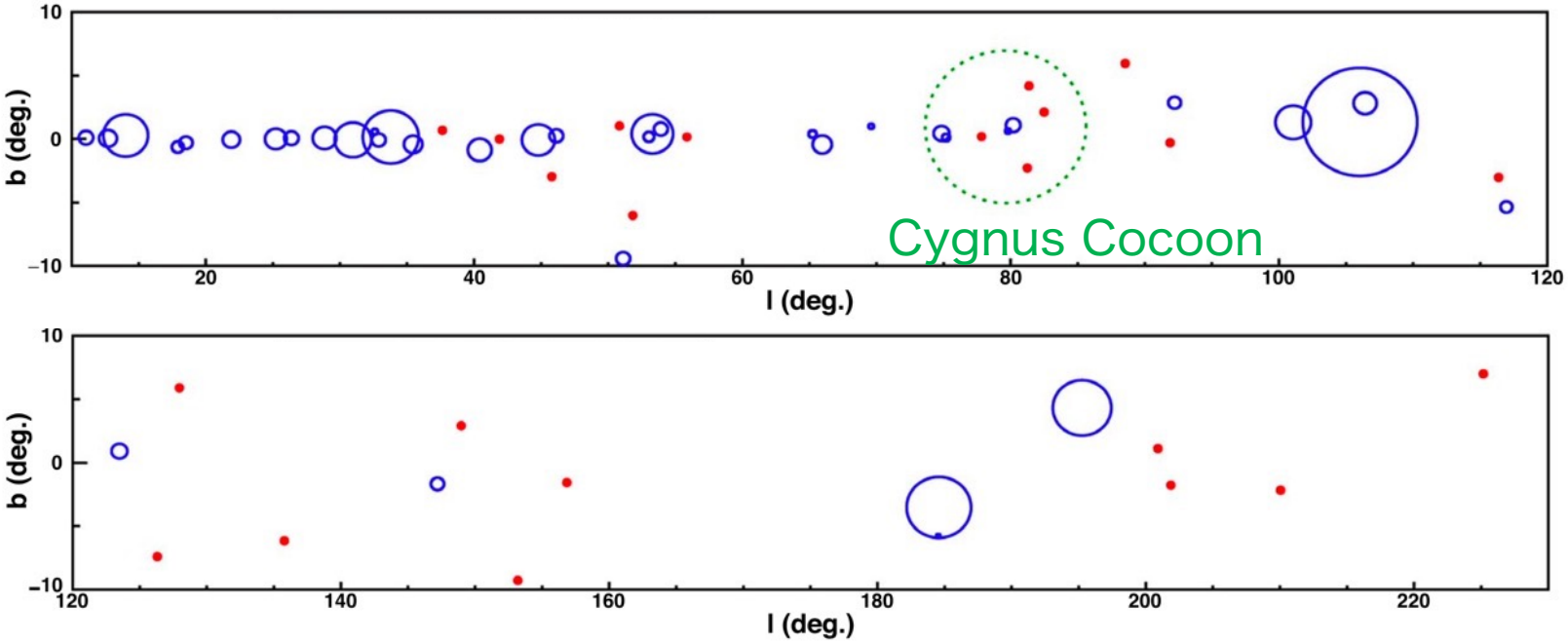

23 Tibet diffuse events (E > 398TeV)
Extension (95% containment) of sub-PeV LHAASO sources

Sub-PeV LHAASO sources covers 3.7% of the ROI.
Expected # of accidental overlap is 23 × 0.037 = 0.9 events
=> Consistent w/ no overlap

Is It Natural to Have No Overlap?

Expected # of γ-ray events observed by Tibet ASγ from the sub-PeV LHAASO sources:

It is calculated for the 22 sub-PeV LHAASO sources not associated w/ the TeVCat sources masked in the Tibet GDE analysis

$$n = F(>398\ \mathrm{TeV}) \times \left(\frac{\int_{\theta<40^\circ} D \cos\theta(t) dt}{\int_{\theta<40^\circ} dt} \right) \times S_{\mathrm{MD}} \times T_{\theta<40^\circ}.$$

F(>398TeV): Integral γ-ray flux
D (=65,700 m^2): Area of the Tibet AS array
$T_{\theta<40^\circ}$: Duration w/i $\theta < 40^\circ$
S_{MD} = 0.3: γ-ray survival ratio @ E > 398 TeV

Sum of n's over the newly-reported sources is 1.2

=> <u>Consistent w/ no overlap</u>

Table 1
List of the Newly Reported Sub-PeV LHAASO Sources

Source Name	δ (deg)	n
1LHAASO J0007+5659u	57.00	2.5×10^{-2}
1LHAASO J0007+7303u	73.07	0
1LHAASO J0056+6346u	63.77	4.7×10^{-2}
1LHAASO J0206+4302u	43.05	7.5×10^{-2}
1LHAASO J0212+4254u	42.91	6.0×10^{-2}
1LHAASO J0216+4237u	42.63	6.3×10^{-2}
1LHAASO J0343+5254u	52.91	3.0×10^{-2}
1LHAASO J1740+0948u	9.81	2.6×10^{-2}
1LHAASO J1809-1918u	−19.30	0
1LHAASO J1814-1719u	−17.89	0
1LHAASO J1814-1636u	−16.62	0
1LHAASO J1825-1256u	−12.94	0
1LHAASO J1825-1337u	−13.63	0
1LHAASO J1839-0548u	−5.8	6.4×10^{-2}
1LHAASO J1959+2846u	28.78	0.12
1LHAASO J1959+1129u	11.49	5.5×10^{-2}
1LHAASO J2002+3244u	32.64	3.8×10^{-2}
1LHAASO J2020+3649u	36.82	0.12
1LHAASO J2031+4052u	40.88	0.10
1LHAASO J2108+5153u	51.90	0.16
1LHAASO J2200+5643u	56.73	5.5×10^{-2}
1LHAASO J2229+5927u	59.55	0.11

n = 0 for sources w/ $|\delta_{src} - \delta_{Tibet}| > 40^\circ$

Source-Origin Hypothesis for Tibet GDE @ > 0.4 PeV

of unresolved sources needed if we assume the source origin of all 23 Tibet GDE events (E > 398 TeV, except for 4 events from the Cygnus Cocoon)

$$22 \times (23 - 4) / 1.2 \times (T_{obs} / T_{obs,0}) = 350\ (T_{obs} / T_{obs,0})\ \text{sources},$$

where

22 = # of sub-PeV γ-ray sources in the 1st LHAASO catalog not detected as of 2021

T_{obs} = Observation time in a future new catalog

$T_{obs,0}$ = Observation time in the 1st LHAASO catalog

$T_{obs} / T_{obs,0} = 2$ => 700 sources

$T_{obs} / T_{obs,0} = 3$ => 1000 sources

LHAASO must detect 8 ~ 10 times more sources in the coming years, IMPOSSIBLE

c.f., Fermi 1st catalog: 1451 sources in 11-month obs.

Fermi 4th catalog: 5064 sources in 8-year obs.

Other Checks

S.K. et al., ApJL 961, L13 (2024)

Let us consider other source catalogs.
A 0.5° circular window is opened for each of the cataloged sources, &
the # of Tibet GDE events w/i the windows is counted.

1. For the 47 1LHAASO sources detected only below 100TeV

   => One Tibet GDE event (TASG-D01-025) overlaps w/ 1LHAASO J1907+0826 &
   consistent w/ accidental overlap (0.19 events)

2. For the latest 92 TeVCat sources w/i the Tibet F.O.V.*

   *As of 2023 December 7th & does not include 1LHAASO sources

   => No overlap & consistent w/ accidental overlap (0.38 events)

Interpretation of the Tibet & LHAASO GDE Fluxes

S.K. et al., ApJL 977, L3 (2024)

$$\frac{\text{Tibet GDE } (25^\circ<l<100^\circ, |b|<5^\circ) - \text{Source}}{\text{LHAASO GDE}^1\ (15^\circ<l<125^\circ, |b|<5^\circ)} = 3,\ 2,\ \&\ 7\ @\ 120\text{TeV},\ 220\text{TeV},\ \&\ 530\text{TeV}$$

LHAAASO masking in the inner Galaxy[1]

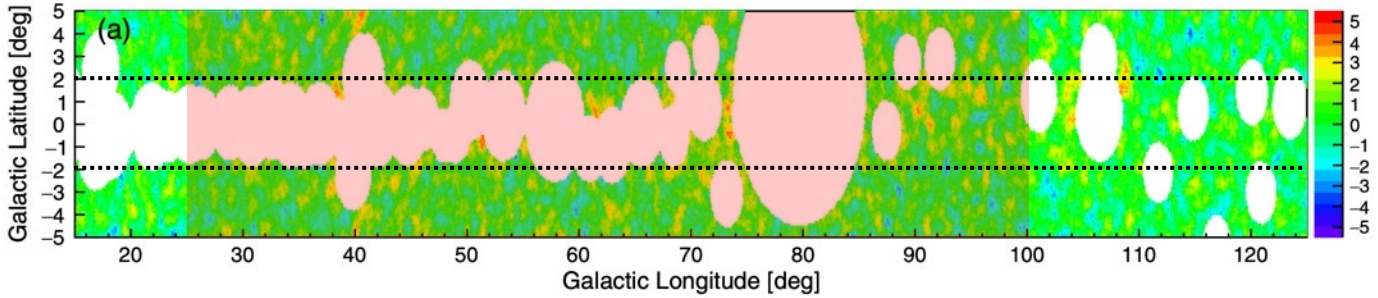

: Tibet region A (25° < l < 100° & |b| < 5°)

LHAASO masks most regions in |b| < 2°
(Tibet masking: ~5% of F.O.V.)

1. Cao et al., PRL 131, 151001 (2023)
2. Lipari & Vernetto, PRD 98, 043003 (2018)

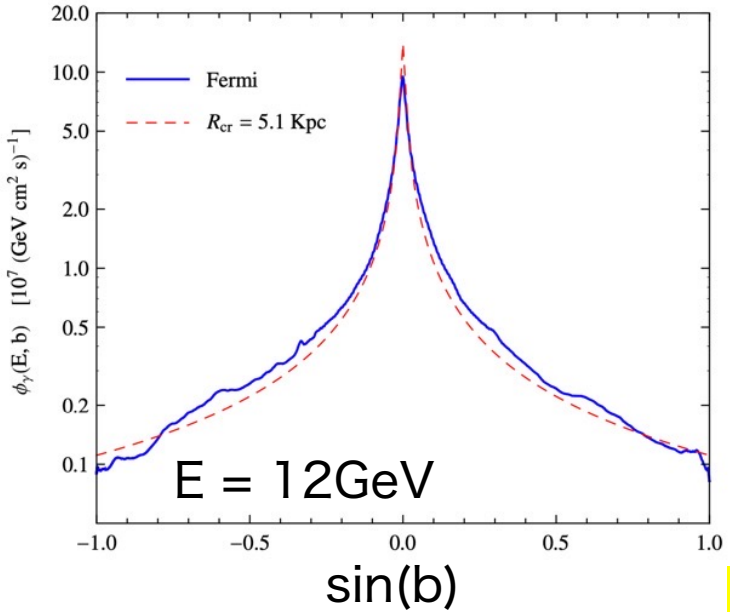

GDE latitudinal distribution* by Lipari & Vernetto (2018)[2]

*The distribution is Integrated over |l| < 180°

Using the theoretical prediction,

Flux(|b|<5°) ÷ Flux(2°<|b|<5°) ~ 3

~ Tibet region A ~ LHAASO inner Gal. plane

The following scenario can explain the difference:
They observe hadronic GDE, but in the different Galactic latitudinal regions due to their different masking schemes

Comparison of Tibet GDE Flux & Not-Masked LHAASO Flux

S.K. et al., ApJ 984, 98 (2025)

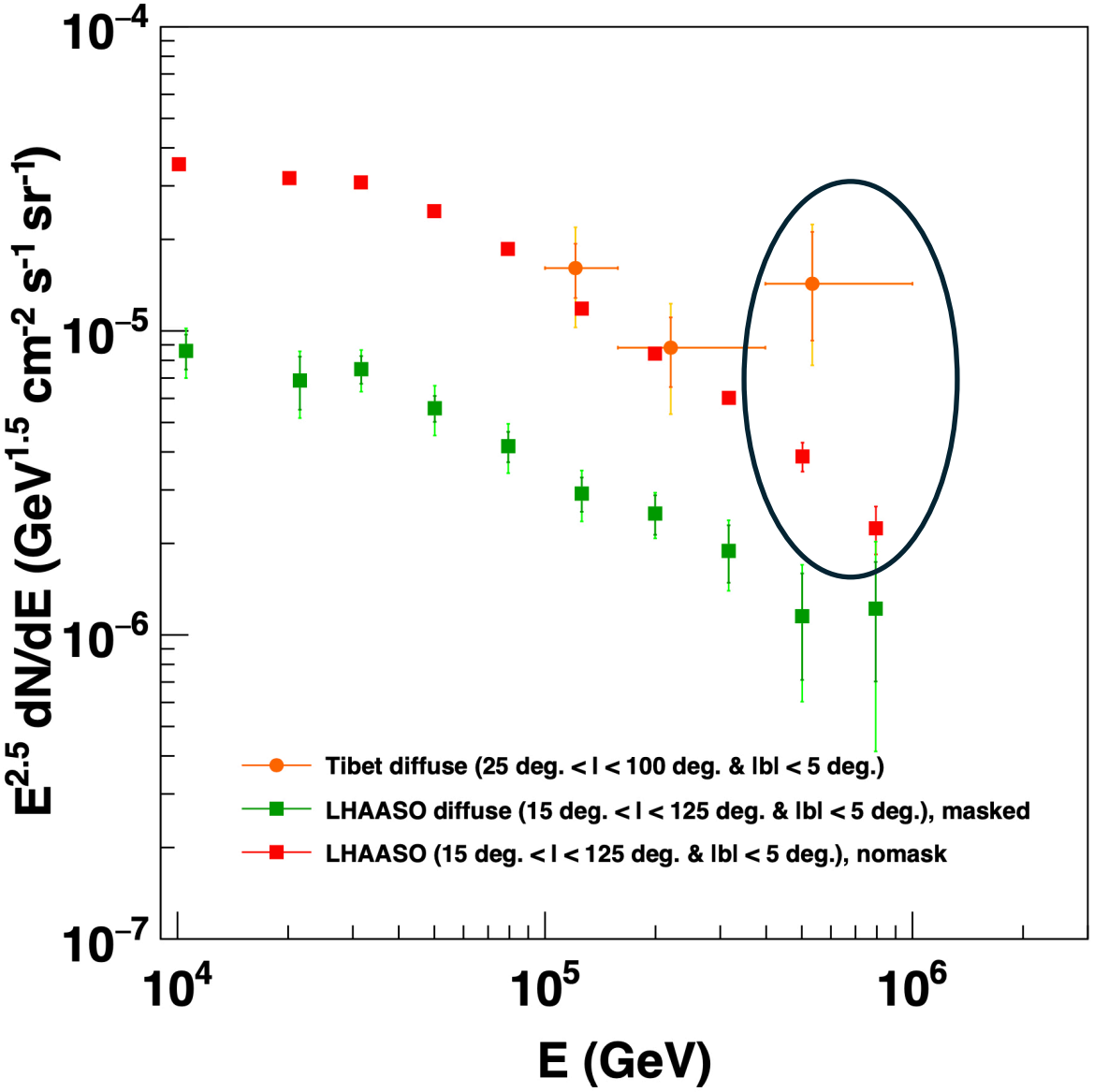

@ E > 400TeV: ~ 2σ statistical deviation

Tibet: 10 events (= 6 + 4 from Cygnus Cocoon)

Consistent w/ statistical fluctuation

Contribution from 1LHAASO @ > 25TeV to the Tibet GDE Flux

S.K. et al., ApJL 977, L3 (2024)

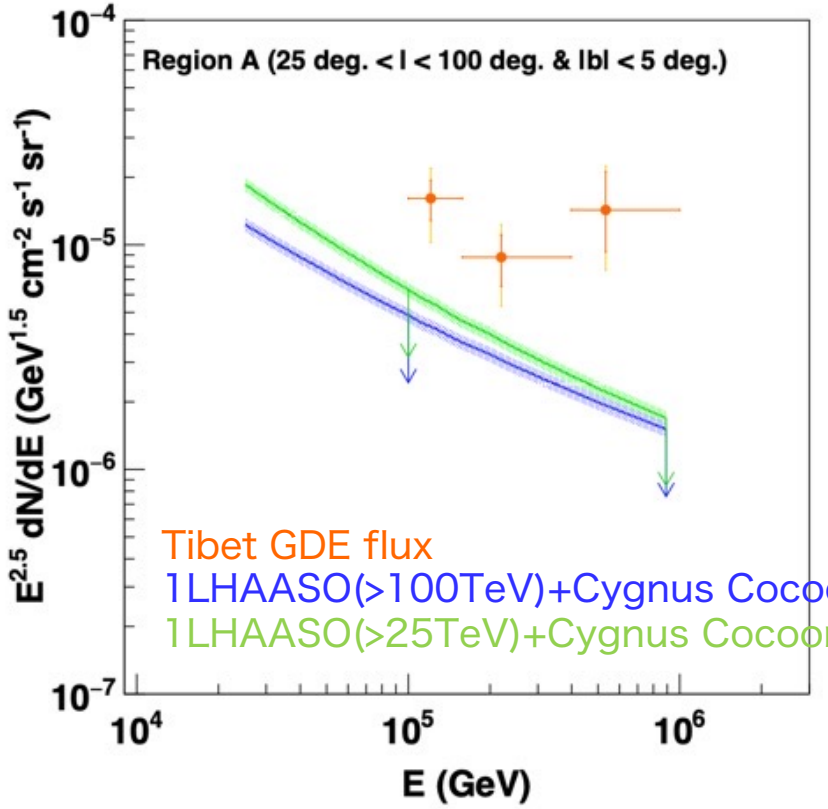

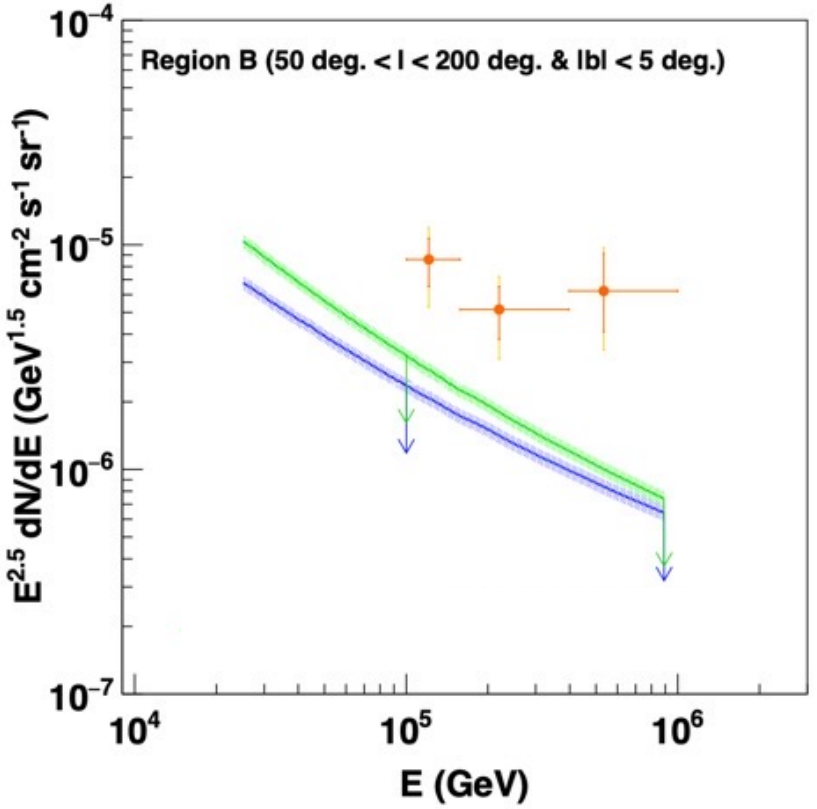

Src/TibetGDE	Region A (25°<l<100° & |b|<5°)	Region B (50°<l<200° & |b|<5°)
121 TeV	< 34.5%±12.7%	< 32.2%±12.7%
220 TeV	< 42.5%±17.1%	< 34.8%±14.2%
534 TeV	$< 15.6\%^{+7.3\%}_{-8.9\%}$	$< 16.1\%^{+7.4\%}_{-9.1\%}$

Contribution from Resolved Leptonic Sources

S.K. et al., ApJL 977, L3 (2024)

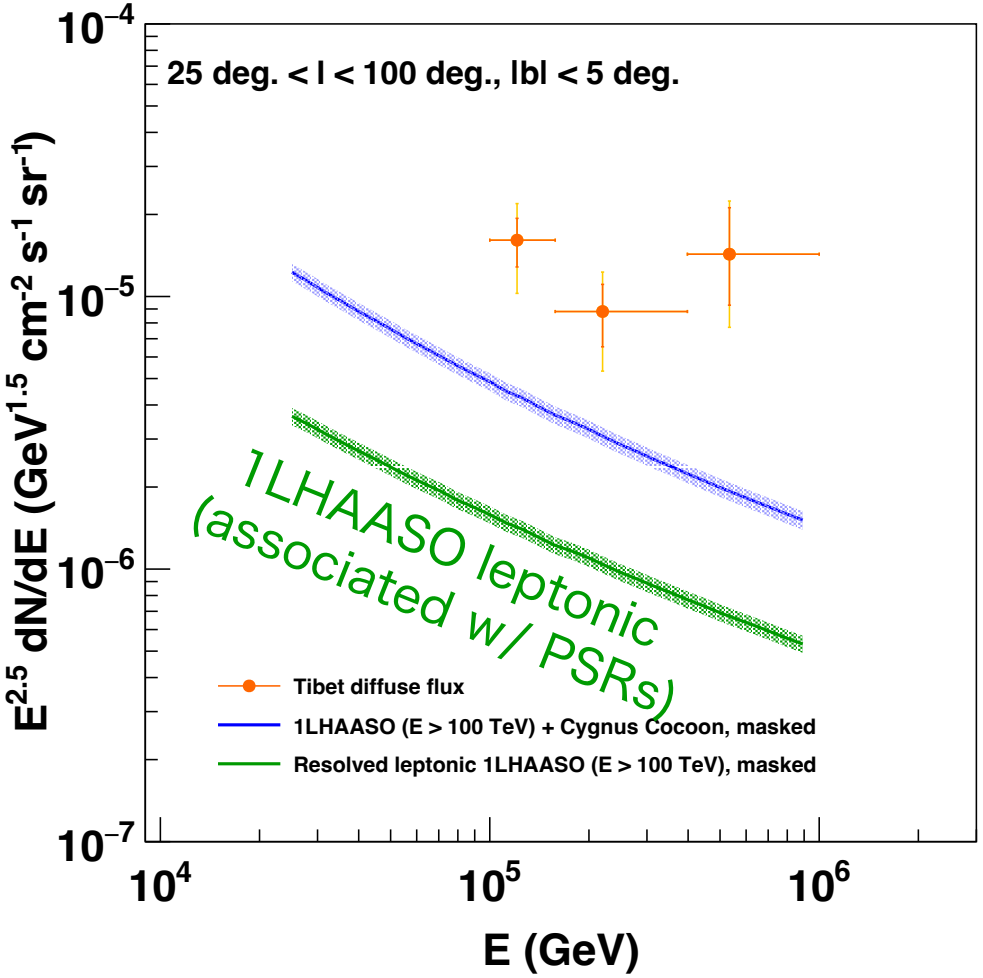

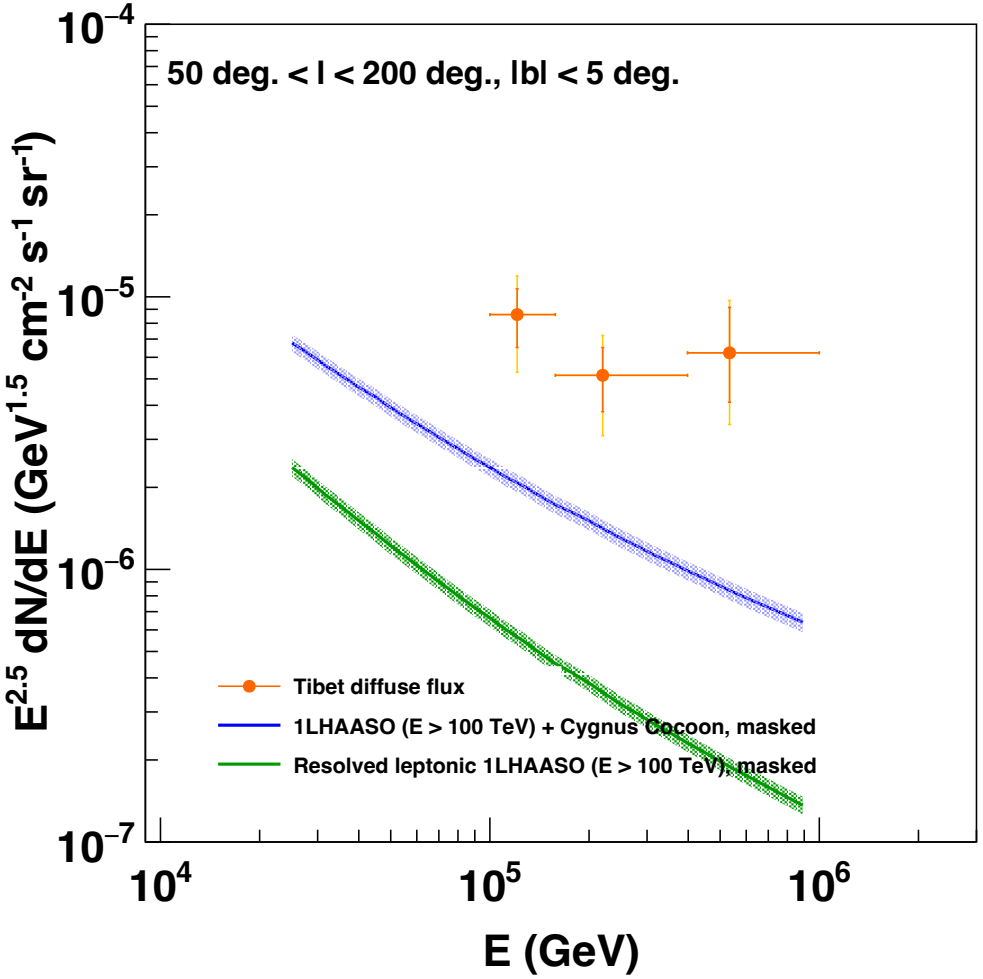

121 TeV	< 8.9%	< 6.6%
220 TeV	< 11.8%	< 6.9%
534 TeV	< 4.7%	< 3.0%

Difference b/w Tibet & LHAASO GDE Fluxes

Sec. 2.2 of Fang & Murase, ApJL 957, L6 (2023)

estimated to be <10%. The innermost Galactic disk at $15° \lesssim l \lesssim 90°$ and $|b| \lesssim 1.°5$ is mostly masked in the study of Cao et al. (2023a), which could have caused an underestimate of the average GDE in that region. Cao et al. (2023a) found that the flux of the GDE of the inner Galaxy ($15° < l < 125°$ and $|b| \lesssim 5°$) would increase by 61% when not apply any masking. The GDE flux of the inner Galaxy measured by LHAASO is slightly lower than that of Tibet ASγ, which could be a result of the more and larger source masks used in LHAASO's analysis. Recently, Li (2023) reports the detection of the

A reason for the difference is suggested by the authors in 2023

Nature of Sub-PeV LHAASO GDE

Fang & Murase, ApJL 957, L6 (2023)

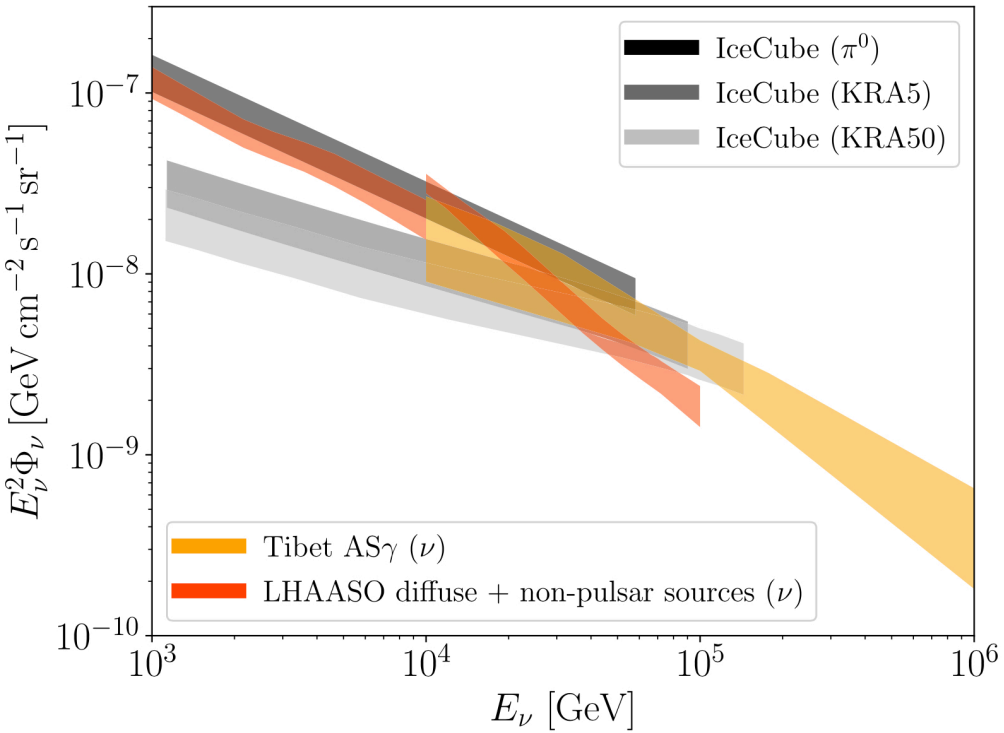

Hadronic diffuse &/or unresolved hadronic

Kaci et al., ApJL 975, L6 (2024)

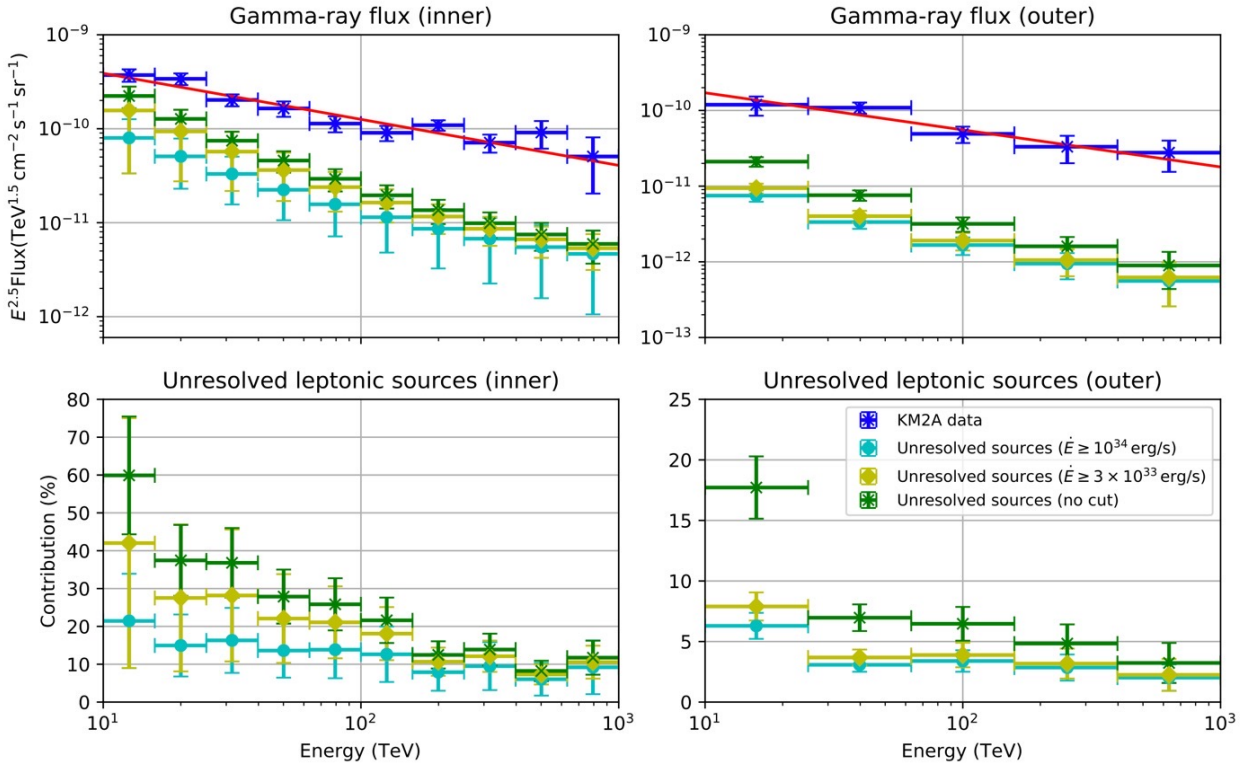

Unresolved leptonic < 20% @ E > 100TeV
=> Hadronic

Hadronic diffuse &/or unresolved hadronic

On the Potential Contribution from Unresolved Sources

Do many unresolved sources w/ hard spectral index avoiding the detection contribute to the Tibet diffuse flux? (e.g., HESS J1702-420A)

However, there is no source like HESS J1702-420A discovered in the northern hemisphere. In fact, if HESS J1702-420A was in the northern hemisphere, LHAASO would easily detect such a source with the current sensitivity.

Therefore, it is not natural to assume that all hard gamma-ray sources potentially situated in the northern hemisphere have fluxes below the current LHAASO sensitivity

One interesting source is 1LHAASO J2031+4052u.

Abdalla et al., A&A 653, A152 (2021)

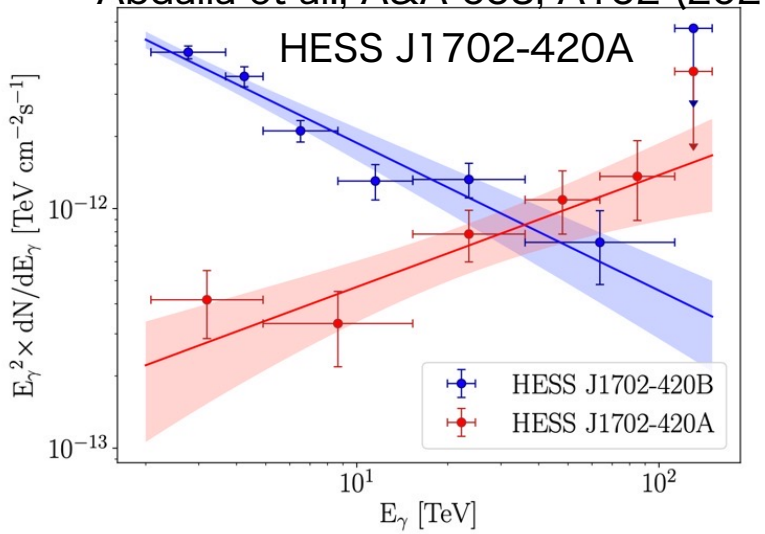

Cao et al., ApJS 271, 25 (2024)

Source Name	Components	α_{2000}	δ_{2000}	$\sigma_{p,95,stat}$	r_{39}	TS	N_0	Γ	TS_{100}	Assoc. (Sep. (deg))
1LHAASO J2031 +4052u*	WCDA	307.90	40.88	0.19	0.25 ± 0.05	57.8	0.77 ± 0.12	2.81 ± 0.16		LHAASO J2032 +4102 (0.20)
	KM2A	308.14	40.88	0.13	<0.08	33.6	0.08 ± 0.02	2.13 ± 0.27	38.4	

Unresolved Source Contribution @ E > 100 TeV

Lipari & Vernetto, PRD 111, 063035 (2025)

- LHAAS GDE ($\Phi_{\text{data, diffuse}}$): masking considered
- The unresolved source contribution ($\Phi_{\text{model, unresolved}}$): masking NOT considered

@ E > 100TeV, the unresolved source contribution should be subdominant.

LHAASO–KM2A Telescope. Energy Interval [100–1000] TeV				
All Sky: $N_{\text{sources}} = 44$ Region A: $N_A = 36$ Region B: $N_B = 8$.				
LHAASO Inner–Galaxy [$(\lvert b\rvert < 5^\circ)$, $(15^\circ \le \ell \le 125^\circ)$]				
$N^{\text{data}}_{\text{sources}} = 30$				
$\Phi^{\text{resolved}}_{\text{sources}} = 3.70 \times 10^{-14}$ [cm^{-2}s^{-1}].				
$\Phi^{\text{data}}_{\text{diffuse}} = (2.09^{+0.43}_{-0.37}) \times 10^{-14}$ [cm^{-2}s^{-1}] (masking sources)				
$\Phi^{\text{data}}_{\text{diffuse}}/\Phi^{\text{resolved}}_{\text{sources}} = 0.56^{+0.12}_{-0.10}$				
LHAASO Outer–Galaxy [$(\lvert b\rvert < 5^\circ)$, $(125^\circ \le \ell \le 235^\circ)$]				
$N^{\text{resolved}}_{\text{sources}} = 3$				
$\Phi^{\text{resolved}}_{\text{sources}} = 0.243 \times 10^{-14}$ [cm^{-2}s^{-1}]				
$\Phi^{\text{data}}_{\text{diffuse}} = (0.92^{+0.32}_{-0.25}) \times 10^{-14}$ [cm^{-2}s^{-1}] (masking sources)				
$\Phi^{\text{data}}_{\text{diffuse}}/\Phi^{\text{resolved}}_{\text{sources}} = 3.8^{+1.2}_{-1.0}$				
Modeling of gamma–ray sources				
	Model 1	Model 2	Model 3	Model 4
Luminosity distribution	Identical sources	Identical sources	P.L. ($\gamma = 1.25$)	P.L ($\gamma = 1.25$)
Space distribution	Smooth (PWN)	Spirals	Smooth (PWN)	Smooth (PWN)
Source size	$R = 0$	$R = 0$	$R = 0$	$R = 20$ pc
Global properties of Galactic gamma–ray sources				
Horizon [kpc]	$10.7^{+5.2}_{-4.6}$	$10.4^{+7.5}_{-3.8}$	$41.5^{+90.}_{-30-.}$	$28.1^{+80.}_{-19.}$
L_0 or L_* [10^{32} erg/s]	$2.6^{+3.1}_{-1.7}$	$2.4^{+4.7}_{-1.4}$	38^{+80}_{-29}	$18.^{+80.}_{-16.}$
L_{tot} [10^{34} erg/s]	$7.6^{+2.9}_{-1.6}$	$6.3^{+5.2}_{-1.5}$	$16.0^{+15}_{-9.1}$	$13.9^{+12}_{-3.6}$
Modeling LHAASO–KM2A ($E > 100$ TeV) Inner–Galaxy region				
$N^{\text{model}}_{\text{Inner}}$	32^{+3}_{-7}	31^{+3}_{-6}	31^{+2}_{-7}	32^{+2}_{-7}
$\Phi^{\text{model}}_{\text{resolved}}$ [10^{-14} (cm^{2}s)$^{-1}$]	$1.5^{+0.9}_{-0.6}$	$1.7^{+1.9}_{-0.7}$	$3.6^{+7}_{-2.5}$	$2.9^{+9}_{-1.6}$
$\Phi^{\text{model}}_{\text{unresolved}}$[$10^{-14}$ (cm^{2}s)$^{-1}$]	$0.39^{+0.22}_{-0.13}$	$0.29^{+0.18}_{-0.13}$	$0.36^{+0.25}_{-0.17}$	$0.57^{+0.71}_{-0.39}$
$f_u = \Phi^{\text{model}}_{\text{unresoled}}/\Phi^{\text{model}}_{\text{all}}$	$0.20^{+0.20}_{-0.13}$	$0.15^{+0.21}_{-0.09}$	$0.09^{+0.27}_{-0.09}$	$0.16^{+0.33}_{-0.12}$
$\Phi^{\text{model}}_{\text{unresolved}}/\Phi^{\text{data}}_{\text{diffuse}}$	$0.19^{+0.27}_{0.13}$	$0.14^{+0.21}_{-0.09}$	$0.17^{+0.27}_{-0.09}$	$0.27^{+0.47}_{-0.03}$
$[\Phi^{\text{data}}_{\text{sources}} f_u/(1-f_u)]/\Phi^{\text{data}}_{\text{diffuse}}$	$0.59^{+0.13}_{-0.13}$	$0.40^{+0.09}_{-0.09}$	$0.23^{+0.6}_{-0.2}$	$0.45^{+0.7}_{-0.4}$
Modeling LHAASO–KM2A ($E > 100$ TeV) Outer–Galaxy region.				
$N^{\text{model}}_{\text{Outer}}$	$6.3^{+2.0}_{-1.4}$	$5.8^{+2.2}_{-1.2}$	$5.6^{+1.6}_{-1.1}$	$5.8^{+1.6}_{-1.2}$
$\Phi^{\text{model}}_{\text{resolved}}$ [10^{-14} (cm^{2}s)$^{-1}$]	$0.70^{+0.29}_{-0.19}$	$0.92^{+0.81}_{-0.19}$	$1.5^{+0.80}_{-0.25}$	$1.2^{+0.72}_{-0.53}$
$\Phi^{\text{model}}_{\text{unresolved}}$ [10^{-14} (cm^{2}s)$^{-1}$]	$0.028^{+0.045}_{-0.015}$	$0.026^{+0.025}_{-0.018}$	$0.045^{+0.055}_{-0.022}$	$0.0.094^{+0.19}_{-0.067}$
$f_u = \Phi^{\text{model}}_{\text{unresolved}}/\Phi^{\text{model}}_{\text{all}}$	$0.038^{+0.088}_{-0.025}$	$0.028^{+0.043}_{-0.034}$	$0.029^{+0.12}_{-0.029}$	$0.071^{+0.22}_{-0.067}$
$\Phi^{\text{model}}_{\text{unresolved}}/\Phi^{\text{data}}_{\text{diffuse}}$	$0.030^{+0.050}_{-0.014}$	$0.029^{+0.050}_{-0.01-}$	$0.048^{+0.070}_{-0.031}$	$0.100^{+0.180}_{-0.062}$
$[\Phi^{\text{data}}_{\text{sources}} f_u/(1-f_u)]/\Phi^{\text{data}}_{\text{diffuse}}$	$0.016^{+0.014}_{-0.011}$	$0.012^{+0.01-}_{-0.010}$	$0.012^{+0.33}_{-0.010}$	$0.31^{+0.068}_{-0.06}$

New On-Going GDE Analysis by LHAASO

Extract RS from DGE

The results shown are taken from Rui Zhang ICRC2025

1. **RS:** Morphology - Gaussian & Spectrum - Power-Law / Log-Parabola
2. **DGE:** Morphology - Planck Dust Map & Spectrum - Power-Law / Log-Parabola
3. **Extension:** RS with extension exceeding a threshold value -> DGE (excluding Geminga, Monogem, and Cygnus)

(RS: resolved sources)

WCDA: Geminga

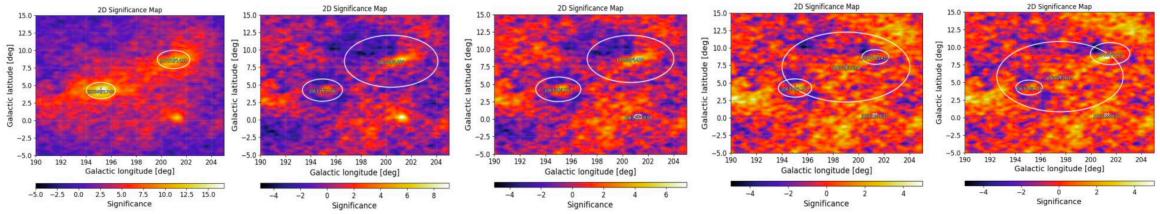

1st LHAASO Cat | refit | +1 source | +2 sources | +3 sources

1st LHAASO Cat:

90 ALL
69 1-25 TeV (> 5σ)
75 > 25 TeV (> 5σ)
43 > 100 TeV (> 4σ)

Galactic Plane (|b|<15 degree):

90 resolved sources, WCDA
90 resolved sources, KM2A
114 resolved sources, JOINT-fit

SED of DGE

INNER

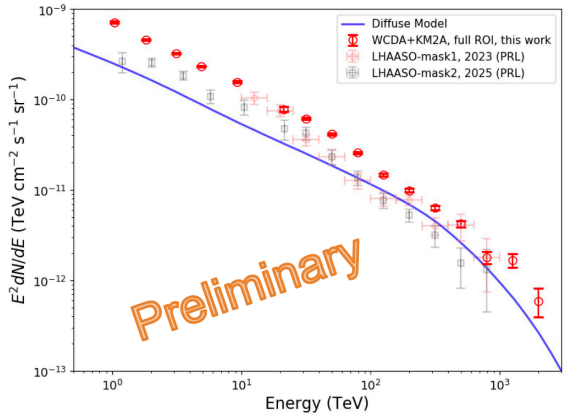

OUTER

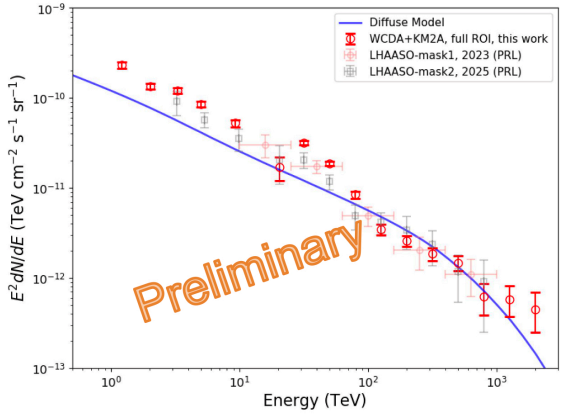

- ✓ Simultaneous modeling of source emission & GDE is now under study
- ✓ Systematic uncertainty in GDE flux from
  - Source spectral shape?
  - GDE emission template (Planck dust map)?
  - Threshold value in extension?
  - LHAASO energy scale uncertainty? …

See Rui Zhang's talk in this session

- **Diffuse Model:** base on LHAASO CR (proton) spectrum (w/o considering Distribution of CRs)
- E < 100 TeV: extra component with Ecut around 100 TeV
- E > 100 TeV: similar spectral shape (index) as that of measurements

Modeling of GDE

Torre Luque et al., arXiv.2507.07083

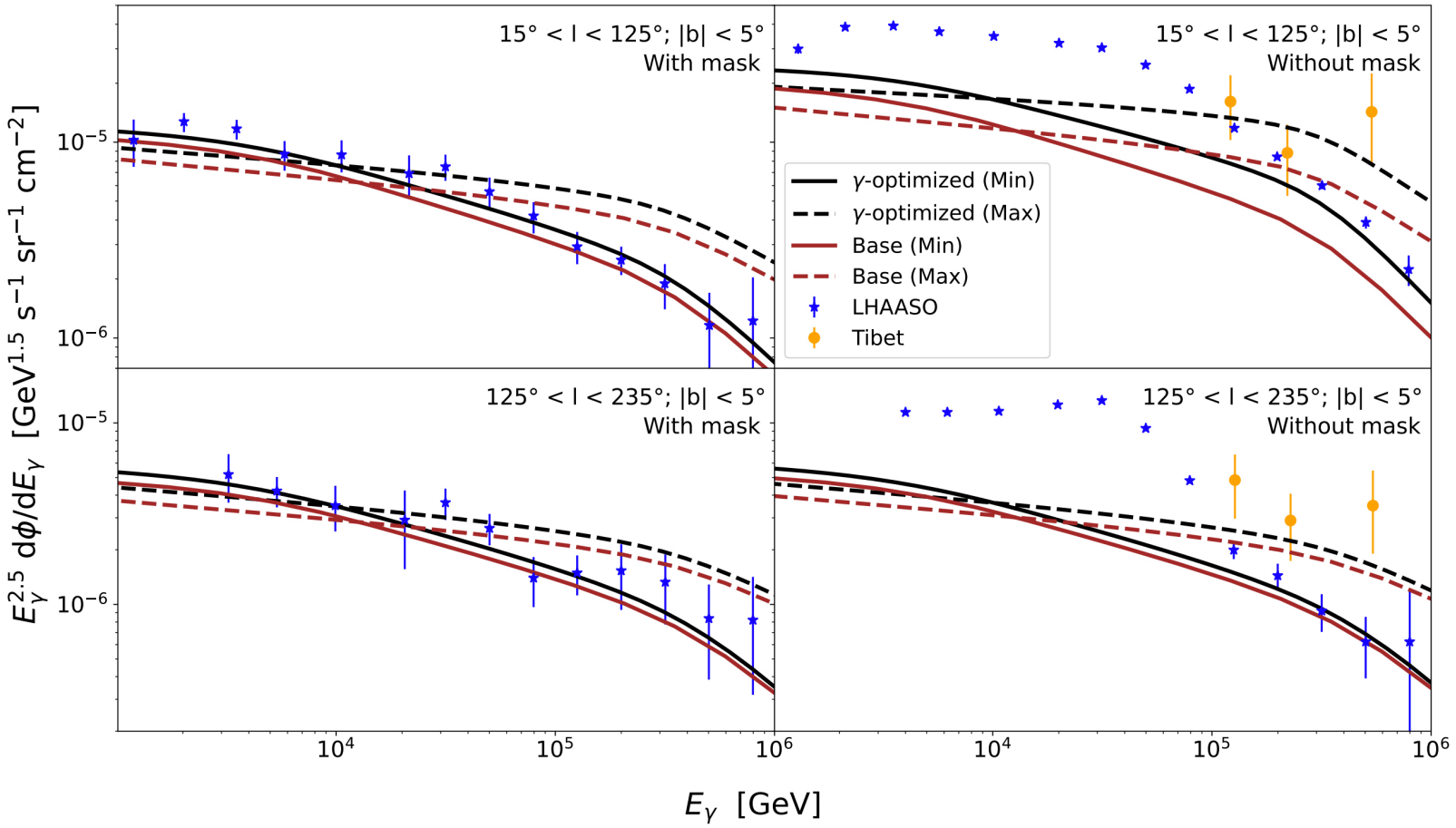

Model/not-masked LHAASO =
2/3 @ 100TeV (γ-optimized, Min)
1/2 @ 100TeV (Base, Min)